myelopathy/tropical spastic paraparesis," *Clinical and Diagnostic Laboratory Immunology*, vol. 6, no. 3, pp. 316–322, 1999.

[109] K. S. Jones, C. Petrow-Sadowski, Y. K. Huang, D. C. Bertolette, and F. W. Ruscetti, "Cell-free HTLV-1 infects dendritic cells leading to transmission and transformation of $CD4^+$ T cells," *Nature Medicine*, vol. 14, no. 4, pp. 429–436, 2008.

[110] P. Jain, S. L. Manuel, Z. K. Khan, J. Ahuja, K. Quann, and B. Wigdahl, "DC-SIGN mediates cell-free infection and transmission of human T-cell lymphotropic virus type 1 by dendritic cells," *Journal of Virology*, vol. 83, no. 21, pp. 10908–10921, 2009.

[111] S. L. Manuel, T. D. Schell, E. Acheampong, S. Rahman, Z. K. Khan, and P. Jain, "Presentation of human T cell leukemia virus type 1 (HTLV-1) Tax protein by dendritic cells: the underlying mechanism of HTLV-1-associated neuroinflammatory disease," *Journal of Leukocyte Biology*, vol. 86, no. 5, pp. 1205–1216, 2009.

[112] S. Rahman, S. L. Manuel, Z. K. Khan et al., "Depletion of dendritic cells enhances susceptibility to cell-free infection of human T cell leukemia virus type 1 in CD11c-diphtheria toxin receptor transgenic mice," *Journal of Immunology*, vol. 184, no. 10, pp. 5553–5561, 2010.

[113] S. Rahman, Z. K. Khan, B. Wigdahl, S. R. Jennings, F. Tangy, and P. Jain, "Murine FLT3 ligand-derived dendritic cell-mediated early immune responses are critical to controlling cell-free human T cell leukemia virus type 1 infection," *Journal of Immunology*, vol. 186, no. 1, pp. 390–402, 2011.

[114] C. R. Nascimento, M. A. Lima, M. J. D. A. Serpa, O. Espindola, A. C. C. Leite, and J. Echevarria-Lima, "Monocytes from HTLV-1-infected patients are unable to fully mature into dendritic cells," *Blood*, vol. 117, no. 2, pp. 489–499, 2011.

Cancer Science
The official journal of the Japanese Cancer Association

T-cell receptor gene therapy targeting melanoma-associated antigen-A4 inhibits human tumor growth in non-obese diabetic/SCID/γc^{null} mice

Yoshitaka Shirakura,[1,2,7] Yukari Mizuno,[1,2,7] Linan Wang,[2] Naoko Imai,[2] Chisaki Amaike,[2] Eiichi Sato,[3] Mamoru Ito,[4] Ikuei Nukaya,[5] Junichi Mineno,[5] Kazutoh Takesako,[5] Hiroaki Ikeda[2,6] and Hiroshi Shiku[1,2,6]

Departments of [1]Cancer Vaccine, [2]Immuno-Gene Therapy, Mie University Graduate School of Medicine, Tsu; [3]Department of Pathology, Tokyo Medical University, Tokyo; [4]Central Institute for Experimental Animals, Kawasaki; [5]Center for Cell and Gene Therapy, Takara Bio Inc., Otsu, Japan

(Received June 20, 2011/Revised September 14, 2011/Accepted September 17, 2011/Accepted manuscript online September 23, 2011/Article first published online November 9, 2011)

Adoptive cell therapy with lymphocytes that have been genetically engineered to express tumor-reactive T-cell receptors (TCR) is a promising approach for cancer immunotherapy. We have been exploring the development of TCR gene therapy targeting cancer/testis antigens, including melanoma-associated antigen (MAGE) family antigens, that are ideal targets for adoptive T-cell therapy. The efficacy of TCR gene therapy targeting MAGE family antigens, however, has not yet been evaluated *in vivo*. Here, we demonstrate the *in vivo* antitumor activity in immunodeficient non-obese diabetic/SCID/γc^{null} (NOG) mice of human lymphocytes genetically engineered to express TCR specific for the MAGE-A4 antigen. Polyclonal T cells derived from human peripheral blood mononuclear cells were transduced with the $\alpha\beta$ TCR genes specific for MAGE-A4, then adoptively transferred into NOG mice inoculated with MAGE-A4 expressing human tumor cell lines. The transferred T cells maintained their effector function *in vivo*, infiltrated into tumors, and inhibited tumor growth in an antigen-specific manner. The combination of adoptive cell therapy with antigen peptide vaccination enhanced antitumor activity, with improved multifunctionality of the transferred cells. These data suggest that TCR gene therapy with MAGE-A4-specific TCR is a promising strategy to treat patients with MAGE-A4-expressing tumors; in addition, the acquisition of multifunctionality *in vivo* is an important factor to predict the quality of the T-cell response during adoptive therapy with human lymphocytes. (*Cancer Sci* 2012; 103: 17–25)

T-cell receptor (TCR) gene transfer using retroviral vectors has been shown to be an attractive strategy to redirect the antigen specificity of polyclonal T cells to create tumor- or pathogen-specific lymphocytes.[1–6] This approach is a promising method for the treatment of patients with malignancies that might overcome the limitations of current adoptive T-cell therapies that have been hampered by difficulties in the isolation and expansion of pre-existing, antigen-specific lymphocytes in patients.[7–10] For the treatment of metastatic melanoma, clinical trials using autologous lymphocytes that have been retrovirally transduced with melanoma/melanocyte antigen-specific TCR have reported objective cancer regression.[11,12] These reports suggest that adoptive cell therapy using TCR gene-modified lymphocytes is a promising approach to immunotherapy in cancer patients; such reports have encouraged the development of novel TCR gene therapy-based approaches.

On-target adverse events, however, have been reported for TCR gene therapies targeting melanocyte differentiation antigens, such as melanoma antigen recognized by T-cells (MART)-1 or gp100. Normal tissues in which melanocytic cells exist, such as the skin, eyes, and inner ears, exhibited severe histological destruction, especially when high-avidity TCR were used.[12] Gene-modified T cells targeting carcinoembryonic antigen also induced a severe transient inflammatory colitis that served as a dose-limiting toxicity for all three patients enrolled.[13] Case reports exploring the severe adverse events seen in patients receiving T cells transduced with chimeric antigen receptors bearing the variable regions of human epidermal growth factor receptor type 2 (HER2)/neu- or CD19-reactive antibodies have suggested that these adverse events might be related to the release of cytokines from transferred cells.[14,15] These observations highlight the potential risk in the usage of receptor genes that render T cells reactive to both tumor cells and a subset of normal cells.

Cancer/testis antigens are particularly attractive targets for immunotherapy, because of their unique expression profiles. While these antigens are highly expressed on adult male germ cells or placenta, they are typically completely absent from other normal adult tissues, and demonstrate aberrant expression in a variety of malignant neoplasms.[16,17] As adult male germ cells do not express MHC class I, $CD8^+$ effector cells theoretically ignore these cells.[18] *MAGE-A*, *-B*, and *-C* genes exhibit such an expression pattern, and their immunogenicity as targets for cancer immunotherapy has been well studied.[19–21] MAGE-A4 expression was reported in 56.6% of serous carcinoma of the ovary, 61.4% of melanoma, 28.4% of non-small cell lung carcinoma, 20% of hepatocellular carcinoma, 22.3% of colorectal carcinoma, 90.2% of esophageal squamous cell carcinoma, and 6.7% of esophageal adenocarcinoma.[22–28] These results suggest that TCR gene therapy targeting the MAGE family of antigens, including MAGE-A4, represents a promising treatment for malignancies that minimizes the risk of severe on-target toxicity. The feasibility of TCR gene therapy targeting MAGE family antigens *in vivo*, however, has not previously been evaluated.

In the present study, we isolated rearranged *TCR$\alpha\beta$* genes from a human $CD8^+$ T-cell clone that recognizes a MAGE-A4-derived peptide, MAGE-$A4_{143-151}$, in the context of HLA-A*2402.[29] Polyclonal human lymphocytes that were retrovirally transduced with these TCR genes demonstrated stable transgene expression and specific cytotoxicity against MAGE-A4-expressing tumor cells *in vitro*.[30,31] These results prompted us to confirm the efficacy of the TCR gene-modified T cells *in vivo* prior to clinical evaluation.

In this study, we investigated if human lymphocytes genetically engineered to express this MAGE-A4-specific TCR could inhibit the growth of MAGE-A4-expressing tumors when adoptively transferred into immunodeficient non-obese diabetic/SCID/γc^{null} (NOG) mice. We evaluated the *in vivo* function of the transferred cells, as well as their migration to the tumor

[6]To whom correspondence should be addressed.
E-mail: shiku@clin.medic.mie-u.ac.jp; hikeda@clin.medic.mie-u.ac.jp
[7]These authors contributed equally to this work.

doi: 10.1111/j.1349-7006.2011.02111.x

site, and the resultant antitumor effect. We addressed if the combination of adoptive cell therapy and vaccination with peptide antigen could influence the antitumor activity of transferred cells.

Materials and Methods

Peripheral blood mononuclear cells. Peripheral blood mononuclear cells (PBMC) were isolated from healthy donors who provided informed consent. Peripheral blood mononuclear cells were cultured in GT-T503 media (Takara Bio, Otsu, Japan) supplemented with 1% autologous plasma, 0.2% human serum albumin (HSA; Sigma-Aldrich, St. Louis, MO, USA), 2.5 mg/mL fungizone (Bristol-Myers Squibb, New York, NY, USA), and 600 IU/mL interleukin-2. This study was approved by the ethics review committees of Mie University Graduate School of Medicine (Tsu, Japan) and Takara Bio.

Mice. Studies were conducted using 8-week-old female NOG mice (Central Institute for Experimental Animals, Kawasaki, Japan) that had been established as described previously.[32] Mice were maintained at the Animal Center of Mie University Graduate School of Medicine. All experimental protocols were approved by the Ethics Review Committee for Animal Experimentation (of Mie University Graduate School of Medicine).

Cell lines. The KE4 (MAGE-A4$^+$HLA-A*2402$^+$ human esophageal carcinoma), QG56 (MAGE-A4$^+$HLA-A*2402$^-$ human lung carcinoma), and T2-A*2402 (human T, B hybridoma transfected with *HLA-A*2402* cDNA)[29] cell lines were maintained in RPMI-1640 media (Sigma-Aldrich) supplemented with 10% FCS, penicillin (100 U/mL), and streptomycin (100 mg/mL).

Retroviral transduction. A retroviral vector encoding MAGE-A4-specific *TCRα* (*TRAV8-1*) and *TCRβ* (*TRBV7-9*) genes (MS-bPa retroviral vector) was described previously.[30] Peripheral blood mononuclear cells were stimulated with 30 ng/mL OKT-3 (Janssen Pharmaceutical, Titusville, NJ, USA) and 600 IU/mL interleukin-2 prior to transduction with MS-bPa particles. Briefly, retroviral solutions were preloaded onto RetroNectin-coated plates and centrifuged at 2000*g* for 2 h, then rinsed with PBS, according to the RetroNectin (Takara Bio)-bound virus infection method. Cells were then applied onto preloaded plates; PBMC transduced with the MS-bPa retroviral vector were designated as gene-modified cells. Control PBMC were treated similarly, except that MS-bPa was omitted from the cultures; these specimens were designated as unmodified cells.

Tumor challenge. KE4 tumor cells (2.5×10^6 in 0.2 mL PBS) were subcutaneously inoculated into the right flanks of mice. In the indicated experiments, QG56 tumor cells (2.5×10^6 in 0.2 mL PBS) were subcutaneously inoculated in a similar manner. Tumor size was determined by the product of perpendicular diameters measured with calipers. The mice were killed before the mean diameter of the tumor reached 20 mm, according to institutional guidelines. The statistical significance of the difference between groups in tumor growth was evaluated at the last time point.

Adoptive cell transfer. After two washes in saline containing 1% human serum albumin (HSA), gene-modified or unmodified cells (1×10^8) were suspended in 0.3 mL saline and intravenously injected into a lateral tail vein of the NOG mice. Prior to injection, gene-modified cells were analyzed for staining with MAGE-A4$_{143-151}$/HLA-A*2402 tetramer and antihuman CD8 mAb to calculate the proportion of tetramer$^+$CD8$^+$ T cells infused. When indicated, HLA-A*2402-positive PBMC were pulsed with 1 μM MAGE-A4$_{141-153}$ peptide and co-administered intravenously as a peptide vaccination.

***In vitro* stimulation and staining of cells.** Cells were incubated for 2 h at 37°C with irradiated (45 Gy) stimulator T2-A*2402 cells, which had been pulsed with 1 μM MAGE-A4$_{141-153}$ or HER2$_{63-71}$ (an irrelevant peptide with HLA-A*2402 binding activity) peptide, at an effector/stimulator ratio of four in the presence of 0.1 mg/mL phycoerythrin (PE)-conjugated anti-CD107a (BD Bioscience, San Diego, CA, USA). We then incubated samples for an additional 6 h in 1 mL/mL GolgiStop (BD Bioscience). The cells were then stained with FITC-conjugated anti-CD8 (BD Bioscience) mAb. After permeabilization and fixation using a Cytofix/Cytoperm kit (BD Bioscience) according to the manufacturer's instructions, the cells were stained intracellularly with allophycocyanin (APC)-conjugated anti-γ-interferon (IFN-γ) (BD Bioscience) and PE–Cy7-conjugated antitumor necrosis factor (TNF) (BD Bioscience) mAb.

Flow cytometric analysis. PE-conjugated MAGE-A4$_{143-151}$/HLA-A*2402 tetramer (provided by the Ludwig Institute for Cancer Research, New York, NY, USA) and FITC-conjugated antihuman CD4 (BD Bioscience), human CD8 (BD Bioscience), and PerCP–Cy5.5-conjugated antihuman CD3 (BD Bioscience) mAb were used to detect transduced TCR in specific cell populations. Polychromatic analyses were performed as previously described.[33] Cell staining data were acquired using a FACS CantoI flow cytometer (Becton Dickinson, Franklin Lakes, NJ, USA), and analyzed using FACSDiva (Becton Dickinson) and FlowJ (Tree Star, Ashland, OR, USA) software.

Immunohistochemical analysis. Formalin-fixed and paraffin-embedded specimens were used. After deparaffinization, tissue sections were pretreated with antigen retrieval solution (DAKO high pH solution, DAKO, Glostrum, Denmark) at 95°C for 20 min. As a primary antibody, antihuman CD8 (clone C8/144B; DAKO) was used. Dextran polymer method with EnVision plus (DAKO) was adopted for secondary detection. 3,3′-Diaminobenzidine was used as chromogen, and hematoxylin counterstain was performed. Infiltrated CD8-positive tumor infiltrating lymphocytes (TIL) were counted in the selected 10 independent areas with most abundant TIL infiltration. Tumor-infiltrated, CD8-positive cells per high power field (0.0625 mm^2) were counted using an ocular grid at ×400 magnification. Three independent counts were performed by a board-certified pathologist (E.S) with no knowledge of the earlier results. The average TIL counts of 10 fields was used for the statistical analyses.

Statistical analyses. Data were expressed as mean ± SD. Differences between groups were examined for statistical significance using the Student's *t*-test. A *P*-value less than 0.01 denoted a statistically-significant difference.

Results

Adoptive transfer of MAGE-A4-specific, TCR-transduced lymphocytes inhibits tumor progression in a dose-dependent and antigen-specific manner. We previously reported the successful retroviral transduction of *TCRαβ* genes recognizing the MAGE-A4$_{143-151}$ peptide in an HLA-A*2402-restricted manner into polyclonally-activated human CD8$^+$ T cells. The TCRαβ-transduced CD8$^+$ T cells exhibited IFN-γ production and cytotoxic activity against both peptide-loaded T2-A*2402 cells and human tumor cell lines, such as KE4, that express both MAGE-A4 and HLA-A*2402.[30] To confirm the efficacy of these gene-modified T cells *in vivo* prior to clinical evaluation, we examined the antitumor efficacy of adoptive cell therapy with MAGE-A4-specific *TCR* gene-modified lymphocytes into NOG mice. We anticipated that a clinical trial to evaluate this therapy would involve the transduction of polyclonally-activated PBMC with *TCR* genes, followed by the transfer of these cells into patients without purification of the CD8$^+$ T-cell subset. To mimic these conditions, the NOG mice received *TCR* gene-modified lymphocytes without further purification. The *TCR* gene-modified and unmodified cells used for the transfer experiments were stained with anti-CD8 mAb and a MAGE-A4$_{143-151}$/HLA-A*2402 tetramer that specifically detected the transduced TCR (Fig. 1A). As we reported previously, this TCR bound the tetramer in a

doi: 10.1111/j.1349-7006.2011.02111.x

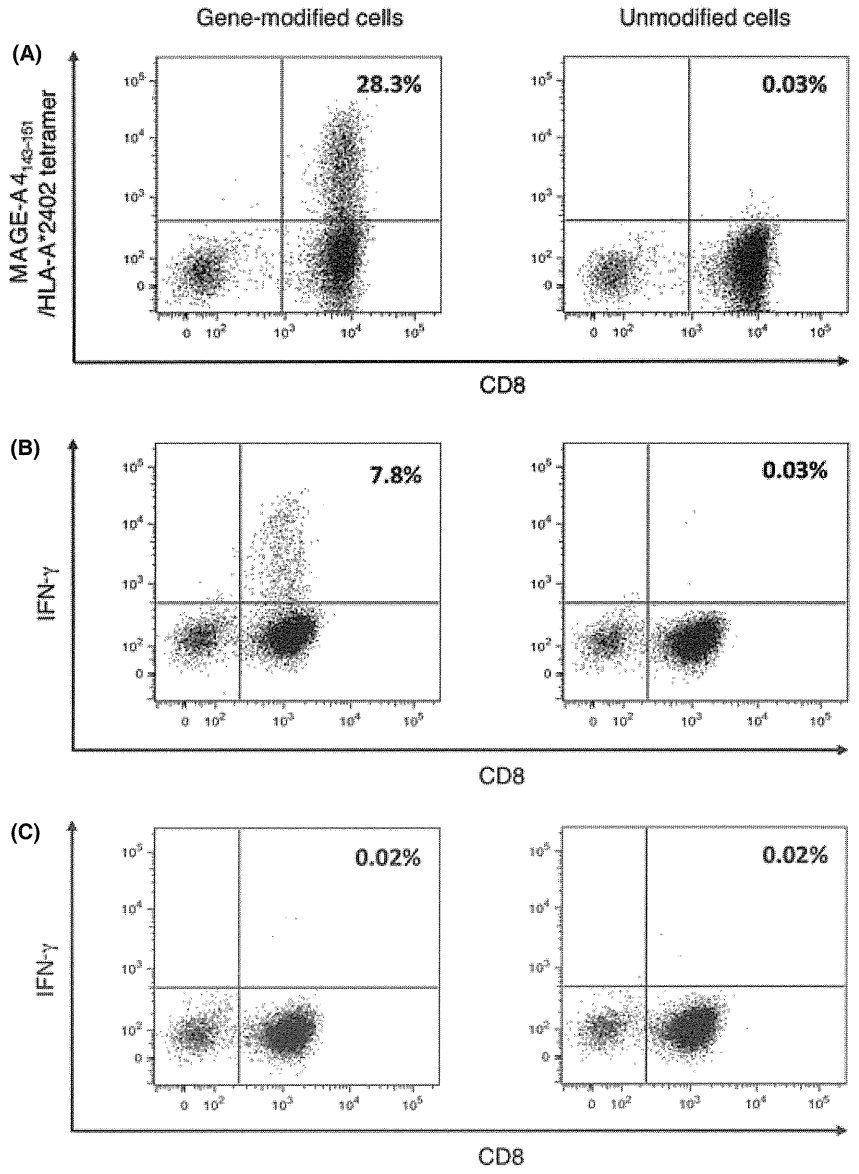

Fig. 1. Transduction of melanoma-associated antigen (MAGE)-A4-specific T-cell receptor (TCR) in human lymphocytes. Peripheral blood mononuclear cells from healthy donors were stimulated with anti-CD3 mAb and interleukin-2. Cells were cultured with or without retroviral vector encoding MAGE-A4-specific TCR, designated gene-modified or unmodified cells, respectively. (A) Representative staining for gene-modified and unmodified cells with MAGE-$A4_{143–151}$/HLA-A*2402 tetramer and antihuman CD8 mAb are shown. (B,C) Gene-modified and unmodified cells were stimulated with T2-A*2402 cells pulsed with the MAGE-$A4_{143–151}$ peptide (B) or HLA-A*2402-binding irrelevant control peptide (C). Representative specific intracellular interferon (IFN)-γ staining is displayed. Numerical value indicates the percentage of the tetramer$^+$ cells or IFN-g$^+$ cells among CD8$^+$ cells.

CD8 molecule-dependent manner.[34] These T cells were tested for specific reactivity against antigen peptide presented on HLA-A*2402 (Fig. 1B,C).

Before transfer, we stained the cells with the MAGE-$A4_{143–151}$/HLA-A*2402 tetramer to calculate the number of tetramer$^+$CD8$^+$ cells. The growth of implanted MAGE-A4$^+$HLA-A*2402$^+$ KE4 tumor cells was significantly inhibited when 9×10^6 of tetramer$^+$CD8$^+$ cells were intravenously injected into NOG mice on day 0 (Fig. 2A). The inhibition of KE4 growth required specific recognition of the MAGE-$A4_{141–153}$/HLA-A*2402 complex by the TCR, because unmodified cells derived from the same donor did not alter KE4 growth. In this experiment, 1×10^8 gene-modified or unmodified lymphocytes derived from the same donor were administered to mice. Although the CD4/CD8 ratio of the *in vitro* expanded lymphocytes depends on the donor, gene-modified and unmodified cells derived from the same donor demonstrated similar phenotypes, determined by the expression of cell surface markers, including CD3, CD4, CD8, CD45RA, CD45RO, CD62L, CCR7, CD152, CD25, CD27, and CD28 (data not shown). The growth of the QG56 tumors, which expressed MAGE-A4, but lacked HLA-A*2402, was indistinguishable in mice receiving either gene-modified or unmodified cells (Fig. 2D). Only a modest inhibition of KE4 growth was seen when mice received only 3×10^6 of tetramer$^+$CD8$^+$ cells (Fig. 2B), while no effect was seen upon administration of 1×10^6 of tetramer$^+$CD8$^+$ cells (Fig. 2C).

We addressed the effect of the adoptive transfer of the gene-modified cells into the mice with established tumors. We adoptively transferred TCR-engineered T cells into NOG mice that were inoculated with KE4 tumor cells 3 days earlier. On the day of adoptive T-cell transfer, we observed the establishment of a KE4 tumor mass in the mice. As shown in Figure 2(E), the administration of gene-modified cells significantly inhibited the growth of KE4 tumors, although the effect was limited and appeared later compared to the treatment on day 0. Taken together, the adoptive transfer of MAGE-A4-specific TCR gene-modified lymphocytes inhibited human tumor growth in NOG mice in a dose-dependent and TCR-specific manner.

Adoptively-transferred human lymphocytes persist in NOG mice. We monitored the persistence of transferred human lymphocytes in peripheral blood by staining Ficoll-purified PBMC from NOG mice with mAb specific for human CD8 and CD4.

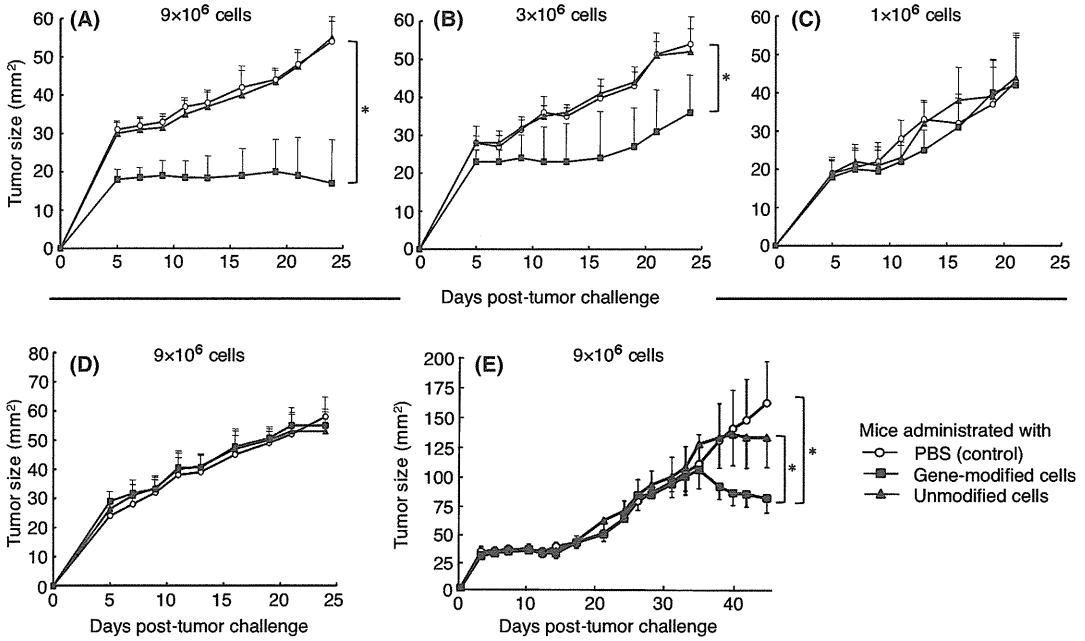

Fig. 2. Adoptive transfer of lymphocytes genetically engineered to express MAGE-A4-specific T-cell receptor inhibits human tumor progression in non-obese diabetic/SCID/γc^{null} mice. Non-obese diabetic/SCID/γc^{null} mice (n = 4 per group) were subcutaneously inoculated with 2.5×10^6 KE4 (A–C) or QG56 (D) tumor cells, and intravenously administered $\sim 1 \times 10^8$ gene-modified (■) or unmodified (▲) cells or PBS alone (control, ○) on day 0. Total of 9×10^6 (A,D), 3×10^6 (B), or 1×10^6 (C) tetramer$^+$CD8$^+$ cells were confirmed to be adoptively transferred; we subsequently monitored tumor growth over time. (E) Non-obese, diabetic/SCID/γc^{null} mice (n = 4 per group) received the treatment 3 days after the subcutaneous inoculation of 2.5×10^6 KE4. Total of 9×10^6 tetramer$^+$CD8$^+$ cells were transferred. Mean tumor size for each group is represented as the average + SD of four mice. Results are representative of three independent experiments. Differences between groups were examined for statistical significance using the Student's t-test. *$P < 0.01$. Numerical value indicates the number of tetramer$^+$CD8$^+$ cells administrated.

Human CD8$^+$ T cells persisted in NOG mice for more than 40 days after transfer (Fig. 3A). The transferred human CD8$^+$ cells comprised between 10% and 30% of the total peripheral mononuclear cells in NOG mice at almost all time points following transfer of 1×10^8 human lymphocytes. In these experiments, approximately 9×10^6 of the transferred 1×10^8 gene-modified cells were tetramer$^+$CD8$^+$. The percentage of specifically staining cells in the total peripheral mononuclear cell population was significantly less when mice received 5×10^7 human lymphocytes (Fig. 3B). There was no significant difference in transferred cell survival or percentages between mice receiving gene-modified and unmodified cells (Fig. 3A,B). Human CD4$^+$ cells comprised less than 10% of all lymphocytes for the first 2 weeks following transfer, but a rapid increase in this population was evident after day 21(Fig. 3C,D). This observation was consistent with reports suggesting that CD4$^+$ T cells play a dominant role in the induction of graft-versus-host (GVH) reactions in hosts receiving transfusions.[35,36] The NOG mice receiving human lymphocyte transfers demonstrated significant weight loss after day 21, a sign of GVH reactions (Fig. 3E).

Transferred TCR gene-modified T cells retain their ability to recognize specific antigens in NOG mice. Lymphocytes harvested from the peripheral blood of NOG mice administered TCR gene-modified lymphocytes were tested for their antigen-specific reactivity by intracellular cytokine staining with anti-IFN-γ mAb after incubation with peptide-loaded T2-A*2402 cells. Antigen-specific IFN-γ secretion was detectable by peripheral blood CD8$^+$ cells isolated from mice throughout the 40-day period after adoptive transfer with either 1×10^8 (Fig. 4A) or 5×10^7 (Fig. 4B) gene-modified cells. No reactivity of these lymphocytes was seen against T2-A*2402 cells without loaded peptide (data not shown). Cells from mice that received unmodified lymphocytes did not demonstrate a specific response (Fig. 4A,B). These results indicate that transferred TCR gene-modified cells remained functional *in vivo*, recognizing the MAGE-A4$_{141-153}$ peptide in the context of HLA-A*2402. When 5×10^7 cells were transferred, these cells expanded more rapidly in the early phase compared to the group with 1×10^8 cells transferred. We speculate that the adoptive transfer of a lower number of antigen-specific T cells might induce these cells to expand more rapidly *in vivo* in the early expansion phase. At the later time points, more antigen-specific cells persisted in mice receiving 1×10^8 cells.

Intratumor infiltration of transferred human CD8$^+$ T cells. To confirm the infiltration of transferred cells into tumor tissue, we examined implanted KE4 and QG56 tumors by immunohistochemical analysis. As antibodies specifically recognizing the transferred TCR (TCRα V8-1 or TCRβ V7-9) are not available, we stained tumor specimens with a mAb against human CD8. Significant infiltration of human CD8$^+$ cells was detectable in KE4 tumors harvested from mice as early as 2 weeks after the transfer of gene-modified cells (Fig. 5A,B). CD8$^+$ cell infiltration in KE4 tumor specimens in the mice that received gene-modified cells was slightly better than in the mice that received unmodified lymphocytes. However, the difference was not statistically significant (Fig. 5A,B). A similar degree of infiltration was also observed in QG56 tumors. These data were consistent with previous reports analyzing the migration of tumor-specific T cells by two-photon laser microscopy that indicated tumor-specific T cells accumulate in both antigen-positive and -negative tumor tissues to comparable extents, but at different migratory velocities, according to tumor antigen expression.[37] The KE4 tumors in mice that did not receive human lymphocytes lacked any positive staining (Fig. 5B).

Combination of TCR gene therapy and peptide vaccine enhances antitumor efficacy. In animal models of adoptive cell therapy examining the effects against murine tumors with tumor-specific CD8$^+$ T cells, *in vivo* vaccinations using agents, such as antigen-peptide or antigen-encoding viruses,

doi: 10.1111/j.1349-7006.2011.02111.x

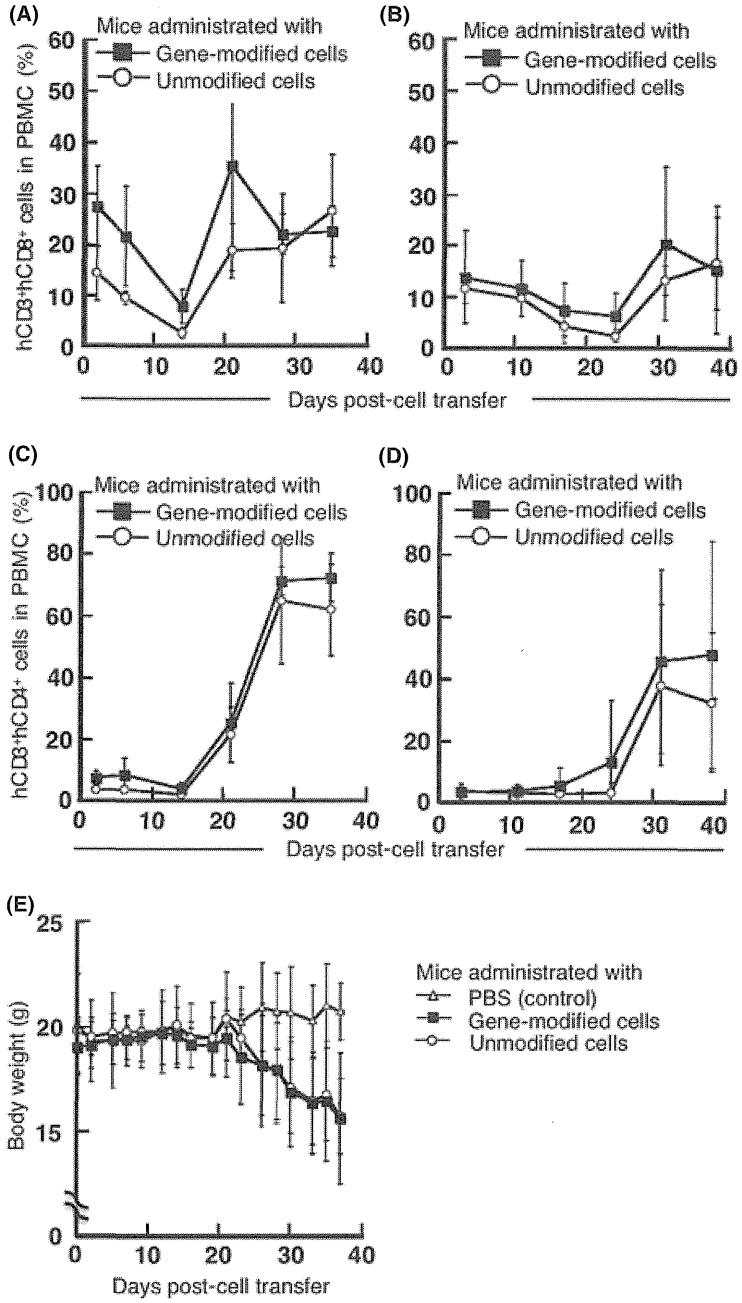

Fig. 3. Persistence of adoptively transferred human lymphocytes in non-obese, diabetic/SCID/γc^{null} (NOG) mice. Non-obese, diabetic/SCID/γc^{null} mice ($n = 4$ per group) were subcutaneously inoculated with 2.5×10^6 KE4 tumor cells, then intravenously administered 1×10^8 (A,C) or 5×10^7 (B,D) gene-modified (■) or unmodified (○) cells on day 0. Mononuclear cells were purified from peripheral blood collected from mice on the indicated days. We evaluated the proportion of human $CD3^+CD8^+$ (A,B) or $CD3^+CD4^+$ (C,D) cells among the mononuclear cell population. (E) We also monitored the body weight of NOG mice administered 1×10^8 gene-modified (■) or unmodified (○) cells or PBS (control, △) over time. Results are representative of three independent experiments. PBMC, peripheral blood mononuclear cells.

can increase the antitumor efficacy of adoptive cell therapy.[9,38] Therefore, we explored if a peptide vaccination in conjunction with TCR gene-modified cell transfer could increase the inhibition of tumor growth seen in this model. As the administration of 1×10^6 $tetramer^+CD8^+$ cells alone was incapable of inducing tumor growth inhibition in this model (Fig. 2C), we examined if the combination of an *in vivo* peptide vaccination with cell transfer under these conditions could enhance tumor inhibition. As NOG mice do not possess endogenous antigen-presenting cells capable of presenting peptide in an HLA-A*2402-restricted manner, we used HLA-A*2402-positive human PBMC pulsed with the MAGE-$A4_{143-151}$ peptide. Tumor-inoculated NOG mice receiving gene-modified cells were also administered peptide-loaded HLA-A*2402-positive PBMC derived from the same donor on days 2 and 8 of the tumor challenge. KE4 tumor growth was significantly inhibited in the mice receiving a combination of cell therapy and peptide vaccination in comparison to mice treated by cell therapy alone (Fig. 6A). The peptide vaccination did not alter KE4 growth when combined with the transfer of unmodified cells. The growth of the HLA-A*2402-negative QG56 tumor was identical in both groups (Fig. 6B).

Increased multifunctionality in adoptively-transferred cells when inoculated with peptide vaccine. We previously reported that the multifunctionality of effector cytotoxic T cells (CTL) is a critical determinant of the quality of the T-cell response and the resultant immunological control of tumor.[33,39] We therefore compared the multifunctionality of transferred cells from NOG mice treated with TCR gene-modified cells and peptide vaccination with that from mice treated by TCR gene cell therapy alone. We assessed IFN-γ and TNF-α production and CD107a mobilization by $CD8^+$ T cells at the single-cell level in specimens harvested from mice on days 2, 7, and 14 after transfer. We

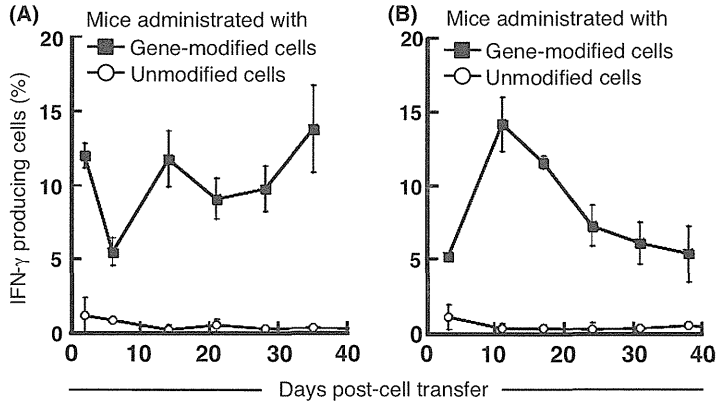

Fig. 4. Lymphocytes genetically engineered to express MAGE-A4-specific T-cell receptor-maintained specific reactivity after *in vivo* passage. Non-obese, diabetic/SCID/γc^{null} mice ($n = 4$ per group) were subcutaneously inoculated with 2.5×10^6 KE4 tumor cells, then intravenously administered 1×10^8 (A) or 5×10^7 (B) gene-modified (■) or unmodified (○) cells on day 0. Mononuclear cells were purified from peripheral blood collected from mice on the indicated days. Intracellular γ-interferon (IFN-γ) production by these cells was assessed after being stimulated with 1 μM MAGE-$A4_{141-153}$ peptide for 6 h. Data are shown as the percentage of IFN-γ-producing cells within the total human $CD8^+$ cell population. Results are representative of three independent experiments.

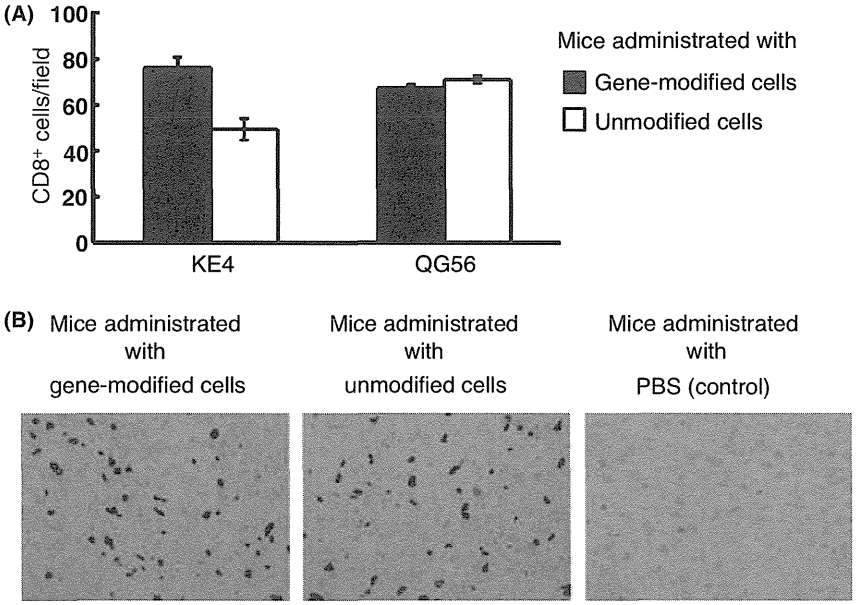

Fig. 5. Adoptively-transferred human $CD8^+$ T cells infiltrate into tumor tissues. Tumor specimens were harvested from non-obese, diabetic/SCID/γc^{null} mice 14 days after subcutaneous inoculation with 2.5×10^6 KE4 or QG56 tumor cells, and intravenous administration of 1×10^8 gene-modified or unmodified cells or PBS (control). We stained formalin-embedded tumor specimens with an antihuman CD8 monoclonal antibody, clone C8/144B. Average $CD8^+$ TIL counts ± SD in KE4 or QG56 (A) and the representative images from KE4 tissue sections (B) are shown.

selected these functional measures because multifunctionality assessed by these factors defines a sensitive correlate of the immunological control of tumors.[33,39]

The mice received human lymphocytes with or without peptide vaccination; isolated peripheral blood specimens were tested for their antigen-specific reactivity of component $CD8^+$ T cells at the indicated time points. On day 2 or 7 after adoptive transfer, we were barely able to detect cells with two or three functions in mice receiving gene-modified cells without peptide vaccination (Fig. 7); cells with three functions comprised 3.7% of all $CD8^+$ T cells, while bifunctional cells comprised 2.4% on day 14. In contrast, mice receiving combination therapy with gene-modified cells and peptide vaccination exhibited a population of cells with three and two functions of 1.4% and 2% of the total $CD8^+$ cells, respectively, as early as day 2. Therefore, multifunctional effector $CD8^+$ T cells appear earlier in mice receiving combination therapy in comparison to those receiving cell therapy alone. On day 7, trifunctional and bifunctional cells in mice receiving combination therapy comprised 1.7% and 4.8% of all cells, respectively. The cells with three or two functions were retained as part of the peripheral mononuclear cell population in these animals on day 14.

Discussion

Successful clinical responses using adoptive cell therapy with tumor-reactive T cells in patients with advanced melanoma have encouraged the development of genetic engineering approaches

doi: 10.1111/j.1349-7006.2011.02111.x

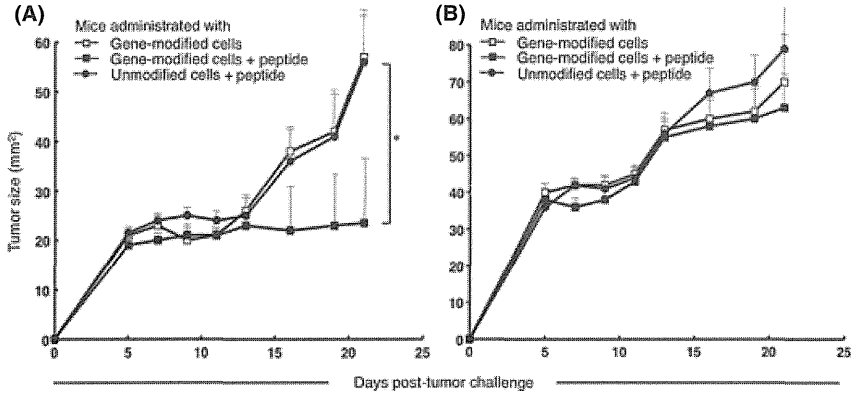

Fig. 6. Peptide vaccination enhanced the antitumor efficacy of adoptive therapy using T-cell receptor, gene-modified cells. Non-obese, diabetic/SCID/γc^{null} mice (n = 4 per group) were subcutaneously inoculated with 2.5×10^6 KE4 (A) or QG56 (B) tumor cells, and intravenously administered 1×10^8 gene-modified (□) or unmodified (●) cells on day 0. Gene-modified population included 1×10^6 tetramer$^+$CD8$^+$ cells. We pulsed 4×10^7 peripheral blood mononuclear cells derived from the same donor (HLA-A*2402 positive) with 1 μM MAGE-A4$_{141-153}$ peptide, and intravenously administered these cells into the animals on days 1 and 8 (■ and ●). Results are representative of three independent experiments.

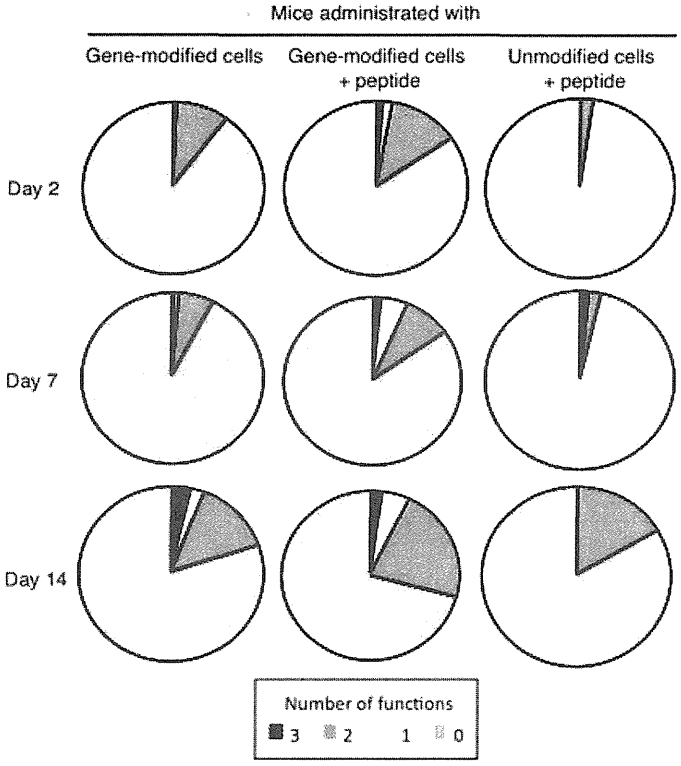

Fig. 7. Peptide vaccination increased the multifunctionality of transferred gene-modified cells. Mice were subcutaneously inoculated with 2.5×10^6 KE4 tumor cells, then intravenously administered 1×10^8 gene-modified or unmodified cells with or without peptide vaccination. Two, 7, and 14 days after transfer, we collected peripheral blood from mice. After purifying the mononuclear cells in these samples, we evaluated their multifunctionality by measuring γ-interferon (IFN-γ) and tumor necrosis factor-α (TNF-α) production and CD107a mobilization. Data are summarized in the pie chart, where each wedge represents the frequency of human CD8$^+$ cells expressing all three functions (3), any two functions (2), a single function (1), or no function (0). Results are representative of three independent experiments.

using patient lymphocytes; these studies aim to extend the range of tumor types that can be treated with this technique and to improve the quality of the lymphocytes employed.[40–42] In a recent clinical trial for metastatic synovial cell sarcoma and melanoma, patients were administered autologous lymphocytes genetically engineered to express a high-avidity TCR against NY-ESO-1; objective clinical responses were observed in four (60%) of six patients with synovial cell sarcoma, and five (45%) of 11 patients with melanoma.[43] In this trial, the transferred TCR contained two amino-acid substitutions in the third complementary determining region of the native TCRα chain that conferred CD8$^+$ T cells with an enhanced avidity. No on-target toxicities were seen in this trial, in contrast to previous observations of vigorous on-target toxicity in patients receiving lymphocytes engineered to express melanocyte differentiation antigen-specific TCR. Genetic engineering also offers the means to endow T cells with enhanced function, as well as resistance to tumor-mediated immunosuppression through the addition of genes encoding homeostatic or pro-inflammatory cytokines,[44,45] chemokine receptors,[46] anti-apoptotic molecules,[47] and costimulatory molecules,[48,49] as well as the silencing of co-inhibitory molecules,[50] although these modifications await clinical evaluation. As increased effector function and/or *in vivo* persistence of cells bearing these modifications might increase on-target toxicity during therapy, the selection of appropriate target antigens is critical to induce favorable antitumor effects and avoid severe adverse events.

The establishment of an animal model suitable for evaluating the *in vivo* efficacy and safety of human adoptive cell therapy is an important challenge to facilitate the development of these therapies and prevent toxicity. Non-obese diabetic/SCID/γc^{null}-immunodeficient mice that lack T, B, and natural killer cells, and demonstrate impaired dendritic cell activity, are a helpful animal model to evaluate the *in vivo* activity of human hematopoietic cells.[32] The NOG mouse model, however, still has limitations, including a homeostatic expansion effect on infused T cells, an allo-reactive response between infused effector cells and transplanted target cells, and potential GVH reactions. In this study, mice receiving human lymphocytes exhibited severe weight loss, consistent with GVH reaction, which worsened after day 21. Therefore, antitumor efficacy in this model is best evaluated before day 21. Future studies will need to evaluate if the homeostatic proliferation of infused cells and/or a suboptimal allo-reactivity influenced the treatment effect seen in this model. The lack of an effect by unmodified cells (Fig. 2) and the increased efficacy upon co-administration of an antigen-peptide vaccine (Fig. 6), however, strongly suggest that the observed antitumor effect was achieved in a MAGE-A4-specific, TCR-mediated manner. The future devel-

opment of improved humanized mice will help to better evaluate the optimization of human immunotherapy.

Multifunctionality is the ability of T cells to exhibit multiple functions, including the simultaneous secretion of multiple cytokines, chemokines, or cytotoxic granules at the single-cell level.[51] The importance of T-cell multifunctionality has been reported in multiple animal infection models[52,53] and in humans infected with HIV, cytomegalovirus, hepatitis B virus, or tuberculosis.[53–60] We reported the importance of effector T-cell multifunctionality in antitumor immune response. Specifically, the appearance of multifunctional $CD8^+$ effector cytotoxic T cells *in vivo* is a critical determinant of effective immunological control of tumors. Regulatory T cells were found to play a role in the inhibition of transferred tumor antigen-specific T-cell multifunctionality.[33,39] In the present study, effector T-cell multifunctionality appeared to correlate with the quality of T-cell responses in adoptive T-cell therapy utilizing genetically-engineered human lymphocytes (Figs 6,7). The peptide vaccination did not significantly change the percentage of human $CD3^+CD8^+$ cells in the PBMC of NOG mice (data not shown). The TCR-transduction efficiency in this study was not very high in general. We found that the combination of vaccination with the adoptive transfer of antigen-specific T cells increased effector T-cell multifunctionality and made the antitumor effect visible, even with a low number of specific TCR-transduced T cells transferred. The unmodified cells with background reactivity were the IFN-γ single producers. We speculate that these cells are positive for IFN-γ because of their non-specific activation due to GVH reaction.

To our knowledge, this study represents the first demonstration *in vivo* of an antitumor effect following the adoptive transfer of human lymphocytes genetically engineered to express a TCR specific for MAGE family antigen. The retroviral vector used in this report is currently under evaluation in a phase I clinical trial designed to treat patients with MAGE-A4-expressing esophageal cancer.

In summary, our data suggest that adoptive cell therapy with human lymphocytes engineered to express MAGE-A4-specific TCR through retroviral transduction is a promising strategy to treat patients with MAGE-A4-expressing tumors. Combination therapy with gene-modified cell-adoptive transfer and *in vivo* vaccination might improve antitumor efficacy, even with low numbers of transferred tumor-reactive T cells. These data support the rationale to explore clinical trials utilizing gene-modified lymphocytes prepared using the vector described in this report.

Acknowledgments

This work was supported by a Grant-in-Aid for Scientific Research from the Ministry of Education, Culture, Sports, Science and Technology of Japan.

Disclosure Statement

No potential conflicts of interest were disclosed.

References

1 Morgan RA, Dudley ME, Yu YY *et al.* High efficiency TCR gene transfer into primary human lymphocytes affords avid recognition of melanoma tumor antigen glycoprotein 100 and does not alter the recognition of autologous melanoma antigens. *J Immunol* 2003; **171**: 3287–95.
2 Rubinstein MP, Kadima AN, Salem ML *et al.* Transfer of TCR genes into mature T cells is accompanied by the maintenance of parental T cell avidity. *J Immunol* 2003; **170**: 1209–17.
3 Zhao Y, Zheng Z, Robbins PF, Khong HT, Rosenberg SA, Morgan RA. Primary human lymphocytes transduced with NY-ESO-1 antigen-specific TCR genes recognize and kill diverse human tumor cell lines. *J Immunol* 2005; **174**: 4415–23.
4 Hughes MS, Yu YY, Dudley ME *et al.* Transfer of a TCR gene derived from a patient with a marked antitumor response conveys highly active T-cell effector functions. *Hum Gene Ther* 2005; **16**: 457–72.
5 Coccoris M, Swart E, de Witte MA *et al.* Long-term functionality of TCR-transduced T cells *in vivo*. *J Immunol* 2008; **180**: 6536–43.
6 Abad JD, Wrzensinski C, Overwijk W *et al.* T-cell receptor gene therapy of established tumors in a murine melanoma model. *J Immunother* 2008; **31**: 1–6.
7 Sadelain M, Riviere I, Brentjens R. Targeting tumours with genetically enhanced T lymphocytes. *Nat Rev Cancer* 2003; **3**: 35–45.
8 Murphy A, Westwood JA, Teng MW, Moeller M, Darcy PK, Kershaw MH. Gene modification strategies to induce tumor immunity. *Immunity* 2005; **22**: 403–14.
9 June CH. Adoptive T cell therapy for cancer in the clinic. *J Clin Invest* 2007; **117**: 1466–76.
10 Rosenberg SA, Restifo NP, Yang JC, Morgan RA, Dudley ME. Adoptive cell transfer: a clinical path to effective cancer immunotherapy. *Nat Rev Cancer* 2008; **8**: 299–308.
11 Morgan RA, Dudley ME, Wunderlich JR *et al.* Cancer regression in patients after transfer of genetically engineered lymphocytes. *Science* 2006; **314**(5796): 126–9.
12 Johnson LA, Morgan RA, Dudley ME *et al.* Gene therapy with human and mouse T-cell receptors mediates cancer regression and targets normal tissues expressing cognate antigen. *Blood* 2009; **114**: 535–46.
13 Parkhurst MR, Yang JC, Langan RC *et al.* T cells targeting carcinoembryonic antigen can mediate regression of metastatic colorectal cancer but induce severe transient colitis. *Mol Ther* 2011; **19**: 620–6.
14 Morgan RA, Yang JC, Kitano M, Dudley ME, Laurencot CM, Rosenberg SA. Case report of a serious adverse event following the administration of T cells transduced with a chimeric antigen receptor recognizing ERBB2. *Mol Ther* 2010; **18**: 843–51.
15 Brentjens R, Yeh R, Bernal Y, Riviere I, Sadelain M. Treatment of chronic lymphocytic leukemia with genetically targeted autologous T cells: case report of an unforeseen adverse event in a phase I clinical trial. *Mol Ther* 2010; **18**: 666–8.
16 Boon T, Old LJ. Cancer tumor antigens. *Curr Opin Immunol* 1997; **9**: 681–3.
17 Scanlan MJ, Gure AO, Jungbluth AA, Old LJ, Chen YT. Cancer/testis antigens: an expanding family of targets for cancer immunotherapy. *Immunol Rev* 2002; **188**: 22–32.
18 Uyttenhove C, Godfraind C, Lethe B *et al.* The expression of mouse gene P1A in testis does not prevent safe induction of cytolytic T cells against a P1A-encoded tumor antigen. *Int J Cancer* 1997; **70**: 349–56.
19 van der Bruggen P, Traversari C, Chomez P *et al.* A gene encoding an antigen recognized by cytolytic T lymphocytes on a human melanoma. *Science* 1991; **254**(5038): 1643–7.
20 De Plaen E, Arden K, Traversari C *et al.* Structure, chromosomal localization, and expression of 12 genes of the MAGE family. *Immunogenetics* 1994; **40**: 360–9.
21 Chomez P, De Backer O, Bertrand M, De Plaen E, Boon T, Lucas S. An overview of the MAGE gene family with the identification of all human members of the family. *Cancer Res* 2001; **61**: 5544–51.
22 Yakirevich E, Sabo E, Lavie O, Mazareb S, Spagnoli GC, Resnick MB. Expression of the MAGE-A4 and NY-ESO-1 cancer-testis antigens in serous ovarian neoplasms. *Clin Cancer Res* 2003; **9**: 6453–60.
23 Peng JR, Chen HS, Mou DC *et al.* Expression of cancer/testis (CT) antigens in Chinese hepatocellular carcinoma and its correlation with clinical parameters. *Cancer Lett* 2005; **219**: 223–32.
24 Li M, Yuan YH, Han Y *et al.* Expression profile of cancer-testis genes in 121 human colorectal cancer tissue and adjacent normal tissue. *Clin Cancer Res* 2005; **11**: 1809–14.
25 Lin J, Lin L, Thomas DG *et al.* Melanoma-associated antigens in esophageal adenocarcinoma: identification of novel MAGE-A10 splice variants. *Clin Cancer Res* 2004; **10**: 5708–16.
26 Tajima K, Obata Y, Tamaki H *et al.* Expression of cancer/testis (CT) antigens in lung cancer. *Lung Cancer* 2003; **42**: 23–33.
27 Yoshida N, Abe H, Ohkuri T *et al.* Expression of the MAGE-A4 and NY-ESO-1 cancer-testis antigens and T cell infiltration in non-small cell lung carcinoma and their prognostic significance. *Int J Oncol* 2006; **28**: 1089–98.
28 Forghanifard MM, Gholamin M, Farshchian M *et al.* Cancer-testis gene expression profiling in esophageal squamous cell carcinoma: identification of specific tumor marker and potential targets for immunotherapy. *Cancer Biol Ther* 2011; **12**: 191–7.

doi: 10.1111/j.1349-7006.2011.02111.x

29 Miyahara Y, Naota H, Wang L *et al.* Determination of cellularly processed HLA-A2402-restricted novel CTL epitopes derived from two cancer germ line genes, MAGE-A4 and SAGE. *Clin Cancer Res* 2005; **11**: 5581–9.
30 Hiasa A, Hirayama M, Nishikawa H *et al.* Long-term phenotypic, functional and genetic stability of cancer-specific T-cell receptor (TCR) alphabeta genes transduced to CD8+ T cells. *Gene Ther* 2008; **15**: 695–9.
31 Okamoto S, Mineno J, Ikeda H *et al.* Improved expression and reactivity of transduced tumor-specific TCRs in human lymphocytes by specific silencing of endogenous TCR. *Cancer Res* 2009; **69**: 9003–11.
32 Ito M, Hiramatsu H, Kobayashi K *et al.* NOD/SCID/gamma(c)(null) mouse: an excellent recipient mouse model for engraftment of human cells. *Blood* 2002; **100**: 3175–82.
33 Imai N, Ikeda H, Tawara I, Shiku H. Tumor progression inhibits the induction of multifunctionality in adoptively transferred tumor-specific CD8+ T cells. *Eur J Immunol* 2009; **39**: 241–53.
34 Hiasa A, Nishikawa H, Hirayama M *et al.* Rapid alphabeta TCR-mediated responses in gammadelta T cells transduced with cancer-specific TCR genes. *Gene Ther* 2009; **16**: 620–8.
35 Bendle GM, Linnemann C, Hooijkaas AI *et al.* Lethal graft-versus-host disease in mouse models of T cell receptor gene therapy. *Nat Med* 2010; **16**: 565–70. 1p following 70.
36 Schroeder ML. Transfusion-associated graft-versus-host disease. *Br J Haematol* 2002; **117**: 275–87.
37 Mrass P, Takano H, Ng LG *et al.* Random migration precedes stable target cell interactions of tumor-infiltrating T cells. *J Exp Med* 2006; **203**: 2749–61.
38 Overwijk WW, Theoret MR, Finkelstein SE *et al.* Tumor regression and autoimmunity after reversal of a functionally tolerant state of self-reactive CD8+ T cells. *J Exp Med* 2003; **198**: 569–80.
39 Imai N, Ikeda H, Tawara I *et al.* Glucocorticoid-induced tumor necrosis factor receptor stimulation enhances the multifunctionality of adoptively transferred tumor antigen-specific CD8+ T cells with tumor regression. *Cancer Sci* 2009; **100**: 1317–25.
40 Dudley ME, Wunderlich JR, Robbins PF *et al.* Cancer regression and autoimmunity in patients after clonal repopulation with antitumor lymphocytes. *Science* 2002; **298**: 850–4.
41 Dudley ME, Wunderlich JR, Yang JC *et al.* Adoptive cell transfer therapy following non-myeloablative but lymphodepleting chemotherapy for the treatment of patients with refractory metastatic melanoma. *J Clin Oncol* 2005; **23**: 2346–57.
42 Dudley ME, Yang JC, Sherry R *et al.* Adoptive cell therapy for patients with metastatic melanoma: evaluation of intensive myeloablative chemoradiation preparative regimens. *J Clin Oncol* 2008; **26**: 5233–9.
43 Robbins PF, Morgan RA, Feldman SA *et al.* Tumor regression in patients with metastatic synovial cell sarcoma and melanoma using genetically engineered lymphocytes reactive with NY-ESO-1. *J Clin Oncol* 2011; **29**: 917–24.
44 Hsu C, Hughes MS, Zheng Z, Bray RB, Rosenberg SA, Morgan RA. Primary human T lymphocytes engineered with a codon-optimized IL-15 gene resist cytokine withdrawal-induced apoptosis and persist long-term in the absence of exogenous cytokine. *J Immunol* 2005; **175**: 7226–34.
45 Liu K, Rosenberg SA. Interleukin-2-independent proliferation of human melanoma-reactive T lymphocytes transduced with an exogenous IL-2 gene is stimulation dependent. *J Immunother* 2003; **26**: 190–201.
46 Kershaw MH, Wang G, Westwood JA *et al.* Redirecting migration of T cells to chemokine secreted from tumors by genetic modification with CXCR2. *Hum Gene Ther* 2002; **13**: 1971–80.
47 Charo J, Finkelstein SE, Grewal N, Restifo NP, Robbins PF, Rosenberg SA. Bcl-2 overexpression enhances tumor-specific T-cell survival. *Cancer Res* 2005; **65**: 2001–8.
48 Topp MS, Riddell SR, Akatsuka Y, Jensen MC, Blattman JN, Greenberg PD. Restoration of CD28 expression in CD28- CD8+ memory effector T cells reconstitutes antigen-induced IL-2 production. *J Exp Med* 2003; **198**: 947–55.
49 Stephan MT, Ponomarev V, Brentjens RJ *et al.* T cell-encoded CD80 and 4-1BBL induce auto- and transcostimulation, resulting in potent tumor rejection. *Nat Med* 2007; **13**: 1440–9.
50 Borkner L, Kaiser A, van de Kasteele W *et al.* RNA interference targeting programmed death receptor-1 improves immune functions of tumor-specific T cells. *Cancer Immunol Immunother* 2010; **59**: 1173–83.
51 Perfetto SP, Chattopadhyay PK, Roederer M. Seventeen-colour flow cytometry: unravelling the immune system. *Nat Rev Immunol* 2004; **4**: 648–55.
52 Chan KS, Kaur A. Flow cytometric detection of degranulation reveals phenotypic heterogeneity of degranulating CMV-specific CD8+ T lymphocytes in rhesus macaques. *J Immunol Methods* 2007; **325**: 20–34.
53 Darrah PA, Patel DT, De Luca PM *et al.* Multifunctional TH1 cells define a correlate of vaccine-mediated protection against Leishmania major. *Nat Med* 2007; **13**: 843–50.
54 De Rosa SC, Lu FX, Yu J *et al.* Vaccination in humans generates broad T cell cytokine responses. *J Immunol* 2004; **173**: 5372–80.
55 Casazza JP, Betts MR, Price DA *et al.* Acquisition of direct antiviral effector functions by CMV-specific CD4+ T lymphocytes with cellular maturation. *J Exp Med* 2006; **203**: 2865–77.
56 Betts MR, Nason MC, West SM *et al.* HIV nonprogressors preferentially maintain highly functional HIV-specific CD8+ T cells. *Blood* 2006; **107**: 4781–9.
57 Precopio ML, Betts MR, Parrino J *et al.* Immunization with vaccinia virus induces polyfunctional and phenotypically distinctive CD8(+) T cell responses. *J Exp Med* 2007; **204**: 1405–16.
58 Beveridge NE, Price DA, Casazza JP *et al.* Immunisation with BCG and recombinant MVA85A induces long-lasting, polyfunctional mycobacterium tuberculosis-specific CD4+ memory T lymphocyte populations. *Eur J Immunol* 2007; **37**: 3089–100.
59 Almeida JR, Price DA, Papagno L *et al.* Superior control of HIV-1 replication by CD8+ T cells is reflected by their avidity, polyfunctionality, and clonal turnover. *J Exp Med* 2007; **204**: 2473–85.
60 Duvall MG, Precopio ML, Ambrozak DA *et al.* Polyfunctional T cell responses are a hallmark of HIV-2 infection. *Eur J Immunol* 2008; **38**: 350–63.

Cellular Immunology 272 (2011) 11–17

Contents lists available at SciVerse ScienceDirect

Cellular Immunology

journal homepage: www.elsevier.com/locate/ycimm

Advantage of higher-avidity CTL specific for Tax against human T-lymphotropic virus-1 infected cells and tumors

Takako Kitazono [a], Takahiro Okazaki [a,*], Natsumi Araya [b], Yoshihisa Yamano [b], Yasuaki Yamada [c], Tatsufumi Nakamura [d], Yuetsu Tanaka [e], Makoto Inoue [a], Shoichi Ozaki [a]

[a] Division of Rheumatology and Allergy, Department of Internal Medicine, St. Marianna University School of Medicine, Kawasaki, Japan
[b] Department of Molecular Medical Science, Institute of Medical Science, St. Marianna University School of Medicine, Kawasaki, Japan
[c] Department of Laboratory Medicine, Nagasaki University Graduate School of Biomedical Science, Nagasaki, Japan
[d] The Department of Molecular Microbiology and Immunology, Nagasaki University Graduate School of Biomedical Science, Nagasaki, Japan
[e] Department of Immunology, Graduate School of Medicine, University of the Ryukyus, Okinawa, Japan

ARTICLE INFO

Article history:
Received 1 August 2011
Accepted 3 October 2011
Available online 8 October 2011

Keywords:
ATL
Avidity
Cytotoxic T-cell (CTL)
HTLV-1
HLA-A2 transgenic mice

ABSTRACT

Strong CTL response can be observed and associated with the control of proviral load in human T-lymphotropic virus type 1 (HTLV-1) infection. However, there are few details with regard to how HTLV-1 specific CTLs work against HTLV-1 infected cells and adult T-cell leukemia cells (ATLs). In this study, using Tax-specific CTL lines with high- and low-functional avidity developed from HLA-A2-transgenic mice, we showed that higher avidity CTLs specific for Tax expressing larger numbers of TCRs and better binding strength to the antigen-HLA-A2 complex are much more efficient at eliminating HTLV-1 infected cells and, in particular, ATL tumor cells with the ability of recognizing a latent level of Tax product detected only with a real-time PCR. These findings suggest that such higher avidity CTLs specific for Tax in HTLV-1 could be responsible for preventing the development of HTLV-1 infection by detecting trace amount of antigens.

1. Introduction

The human T-lymphotropic virus type 1 (HTLV-1) causes two distinct types of disease: a $CD4^+$ T cell malignancy known as adult T cell leukemia (ATL) [1,2] and a range of inflammatory disease, of which HTLV-1-associated myelopathy/tropical spastic paraparesis (HAM/TSP) is the best recognized and most widely studied [3,4]. In patients with HTLV-1 infection, the proviral load of HTLV-1 is usually stable over time [5]. However, the factors determining the set point of proviral load in each person remain to be elucidated. In particular, CTLs are active in individuals with low proviral load, in whom immunosurveillance could be more effective [6,7]. Several studies have reported that high-levels of HTLV-1-specific CTL activity can be observed in HAM/TSP patients and some asymptomatic HTLV-1 carriers, while ATL patients apparently lack HTLV-1-specific CTL activity, although it can be sporadically induced during the remission stages or after mitogenic stimulation with multiple in vitro antigenic stimulations of peripheral blood mononuclear cells [8,9]. One of the major target antigens by HTLV-1-specific CTLs in human is Tax protein [10,11], which is a molecule responsible for T-cell immortalization [12,13]. CTLs induced in ATL patients in remission are able to lyse autologous tumor cells in vitro [14]. These observations suggest that HTLV-1-specific CTLs could play a critical role in host immunosurveillance against ATLs.

While the number of HTLV-1-specific CTLs elicited is unquestionably important [7], recent studies have identified an additional parameter, functional avidity, as critical in determining the efficiency of viral clearance [15–18]. T-cell avidity is a measure of the sensitivity of T cells recognizing a cognate antigen. High-avidity CTLs are those that can recognize antigen-presenting cells (APCs) bearing very low levels of peptide-major histocompatibility complex (MHC) antigen, whereas low-avidity CTLs require much more peptide-MHC antigen to be activated or to exert effector function [15,19–21].

In this study, in order to clarify whether Tax-specific CTLs with higher avidity are critical as a deterrent to control the proliferation of ATL and the expansion of HTLV-1 infection, we developed two CTL lines specific for Tax11-19 antigen having high- and low-avidity from HLA-A2 transgenic mice in vitro. Using these CTLs, we demonstrate not only that Tax product is a critical antigen but also in particular that the specific CTLs with higher avidity for Tax11-19 have a selective advantage on recognition of human ATLs and HTLV-1 infected cells compared with those with low avidity in vitro.

* Corresponding author. Address: Division of Rheumatology and Allergy, Department of Internal Medicine, St. Marianna University School of Medicine, 2-16-1 Sugao, Miyamae-ku, Kawasaki, Kanagawa 216-8511, Japan. Fax: +81 44 977 8593.
E-mail address: okazakit@marianna-u.ac.jp (T. Okazaki).

0008-8749/$ - see front matter © 2011 Elsevier Inc. All rights reserved.
doi:10.1016/j.cellimm.2011.10.002

2. Materials and methods

2.1. Synthetic peptides

The Tax11-19 peptide, LLFGYPVYV, was purchased from Asahi Technoglass (Chiba, Japan) and used as an HLA-A2-restricted CTL antigen [11].

2.2. Cells

C1R.AAD cell line (HMYC1R transfected with HLA chimeric molecule containing α1 and α2 domains from human HLA-A2.1 and α3 from mouse H-2D^d) was described previously [22]. Cell lines were maintained in culture medium (CTM; 1:1 mixture of RPMI 1640 and Eagle-Hank's amino acid (EHAA)) containing 10% fetal bovine serum (FBS), 1 mM sodium pyruvate, 0.1 mM nonessential amino acids, 10 mM HEPES, 4 mM glutamine, 100 U/ml penicillin, and 100 μg/ml streptomycin.

HTLV-1-infected human ATL cell lines, KK-1 and KOB, were derived from the peripheral blood and ascites of ATL patients, respectively [23,24]. Human IL-2 dependent T cell line (HCT-4) was derived from the cerebrospinal fluid of a HAM/TSP patient [25]. KK-1, KOB, and HCT-4 were used as a target. Cells were maintained in CTM with 100 units/ml of recombinant human IL-2 (Imunace®35, Shionogi, Osaka, Japan).

2.3. Mice

Transgenic HHD-2 mice (gift from Dr. François Lemonnier, Institute Pasteur, Paris, France) were bred in our colony at the Institute of the Experimental Animals at St. Marianna University. HHD-2 mice are characterized by knock-out of the murine β_2-microglobulin gene, as well as murine H-2D^b, transgenic expression of human HLA-A2.1 with a covalently-linked human β_2-microglobulin and a murine D^b-derived α3 domain to allow interaction with mouse CD8 [26]. All animal studies were approved by the Institute of Experimental animals at St. Marianna University.

2.4. Binding assay

Peptide binding to HLA-A2 molecules was measured using T2 mutant cell lines as described previously [27,28]. T2 cells (3×10^5/well) were incubated overnight in 96-well plates with culture medium (a 1:1 mixture of RPMI 1640 and Eagle-Hank's amino acid (EHAA) containing 2% FBS, 100 U/ml penicillin, 100 mg/ml streptomycin) with 10 μg/ml human β_2-microglobulin (Sigma–Aldrich, St. Louis, MO) and different peptide concentration. On the following day, cells were washed at 190 × *g* for 5 min twice with cold PBS containing 2% FBS and incubated for 30 min at 4 °C with anti-HLA-A2.1 BB7.2 mAb (1/100 dilution of hybridoma supernatant) and 5 μg/ml FITC-labeled goat anti-mouse Ig (BD PharMingen, San Diego, CA). Cells were washed twice after each incubation; subsequently, HLA-A2.1 expression was measured by flow cytometry (FACScan; BD Biosciences, Mountain View, CA). HLA-A2.1 expression was quantified as fluorescence index (FI) according to the formula: FI = ((geometric mean fluorescence with peptide – geometric mean fluorescence without peptide)/geometric mean fluorescence without peptide). $FI_{0.5}$ is the concentration required to give an FI of 0.5, meaning a 50% increase in HLA-A2 on the cell surface. Background fluorescence without BB7.2 was subtracted for each individual value. To compare the different peptides, $FI_{0.5}$ was calculated from the titration curve for each peptide. Each sample was tested in triplicate. Values were expressed as mean in triplicate.

2.5. CTL generation in HHD-2 transgenic mice

The method for generating antigenic peptide-specific CTL lines form HHD mice was described previously [28,29]. Mice aged more than 8 weeks were immunized subcutaneously in the base of the tail with 100 μl of an emulsion containing 1:1 incomplete Freund's adjuvant (IFA), antigenic CTL peptide and cytokines (50 nmol Tax (11-19) peptide, 25 nmol HBV core 128–140 helper epitope, 3 μg of rmIL-12 and 3 μg of rmGM-CSF). Mice were boosted 2 weeks later, with the spleens removed 10–14 days after the boost. Immune spleen cells (2.5×10^6/well) were stimulated in 24-well plates with autologous spleen cells (5×10^6/well) pulsed for 30 min with 10 μM Tax11-19 peptide for the development of low-avidity CTL lines (LCTL) or with 10 nM for high-avidity CTL lines (HCTL) in CTM supplemented with 10% T-stim® (Collaborative Biochemical Products, Bedford, MA). Following a minimum of four in vitro stimulations with the peptide-pulsed syngeneic spleen cells, two CTL lines were maintained by weekly restimulation with 1×10^6 cells/well with 4×10^6 peptide-pulsed mitomycin C-treated syngeneic spleen cells as feeders.

2.6. Cytotoxic assay

CTL activity was measured with ^{51}Cr-labeled target cells. Target cells (1×10^6) were pulsed in 100 μl of 150 μCi ^{51}Cr for 1 h and were washed three times, with 5000 cells/well then added to 96-well round-bottom plates containing different peptide concentrations. Effector cells were introduced followed by additional incubation. Supernatants were then harvested and analyzed. The percentage of specific ^{51}Cr release was calculated as 100 × (experimental release – spontaneous release)/(maximum release – spontaneous release). Spontaneous release was determined from target cells that had been incubated in the absence of effector cells, while maximum release was determined in the presence of 2% TRITON® X-100 Detergent (CALBIOCHEM, La Jolla, CA). Each sample was tested in triplicate. Values were expressed as means ± SEM of triplicates.

2.7. IFN-γ ELISA assay

IFN-γ in the culture supernatant harvested at 24 h was determined using an ELISA kit (R&D, Minneapolis, MN) according to the manufacture's instructions. All samples were analyzed in triplicate. Values were expressed as means ± SEM of triplicates.

2.8. TCR Vβ screenings of CTLs

We assessed a Vβ usage pattern between HCTL and LCTL using Vβ TCR screening kit by a flow cytometry analysis (BD Bioscience Phamingen, San Diego, CA).

2.9. Flow cytometry

We used a PE-Tax11-19/HLA-A*0201 tetramer-LLFGYPVYV (Medical & Biological Laboratories, Nagoya, Japan) and PE-hamster anti-mouse CD3ε Ab (145-2C11, BD Bioscience Phamingen, San Diego, CA). Cells were centrifuged and washed twice with PBS containing 0.5% BSA, and then resuspended in 1% BSA/PBS. Cells were incubated 40 min at 4 °C with the antibody and then washed three times. The tetramer and anti CD3ε Ab were titrated for staining simultaneously.

In order to compare the affinity of T cell receptor between HCTLs and LCTLs, indexes were calculated using the following two equations: ratio of geometric mean (RGM) = (geometric mean using tetramer or anti-CD3ε Ab)/(geometric mean using control Ab). Each sample was tested in triplicate.

2.10. Western blotting

KK-1, KOB, and HCT-4 were lysed using standard lysis buffer (20 mM Tris–HCl, 250 mM NaCl, 1% NP-40, 1 mM dithiothreitol, 10 mM NaF, 2 mM Na_3VO_4, 10 mM $Na_4P_2O_7$, and protease inhibitor cocktail (Roche, Mannheim, Germany)). Lysates were stored at −80 °C until use. Protein concentration was determined using the Bradford method (Bio-Rad protein assay reagent; Bio-Rad laboratories, Hercules, CA). Equal amounts (30 μg) of protein were separated by SDS–PAGE on 10% polyacrylamide gels and transferred to PVDF membranes. Following the transfer, membranes were blocked with Difco Skim milk (BD Bioscience, San Diego, CA) overnight at 4 °C. The working concentrations of the first Abs were 1 μg/ml for anti-Tax Ab (Lt-4) [30] and anti murine β-actin Ab (SIGMA, St. Louis, MO), and 1:10,000 for HRP-conjugated anti-mouse IgG Ab (SIGMA, St. Louis, MO). The membrane was washed, and was reacted with the appropriate second antibody. Finally, signals were visualized using the extended cavity laser (ECL) system (GE Healthcare Bio-sciences KK, Tokyo, Japan).

2.11. Real-time reverse transcriptase-PCR (RT-PCR)

Total RNA was isolated from cells using TRIzol® Reagent (Invitrogen, Carisbad, CA). First-stand cDNA was synthesized with random hexamers and reverse transcriptase (ReverTraAce; Toyobo, Japan) using 1 μg of total RNA in a reaction volume of 20 μl. Real-time PCR reactions were carried out using TaqMan® Universal Master Mix (Applied Biosystems, Carisbad, CA). ABI Prism 7500 SDS was programmed to an initial step of 2 min at 50 °C and 10 min at 95 °C, followed by 45 cycles of 15 s at 95 °C and 1 min at 60 °C. The primers and probe for detecting the HTLV-1 Tax or GAPDH mRNA were used as described previously [31]. Relative quantification of mRNA was performed using the comparative threshold cycle method with GAPDH as an endogenous control. For each sample, target gene expression was normalized against the expression of GAPDH. To determine relative expression levels, the following formula was used: target gene expression = $2^{-(Ct[target]-Ct[GAPDH])}$. Each sample was tested in triplicate. Values were expressed as means ± SEM of triplicates.

3. Results

3.1. Binding affinity of Tax11-19 for HLA-A2 molecule

Before attempting to develop Tax-specific CTL lines from HLA-A2 transgenic HHD mice, we evaluated the binding affinity of Tax11-19 peptide by T2 binding assay, which measures the cell surface stabilization of HLA-A2 molecules. Tax11-19 peptide displayed a binding capacity for the HLA-A2 molecule that was nearly equal to that of the positive control, the highly antigenic influenza virus matrix peptide (FMP58-66) [32] ($FI_{0.5}$ = 0.329 for Tax11-19, 0.284 μM for FMP58-66) (Fig. 1). These data suggest that Tax11-19 would be a very strong antigenic peptide restricted to the HLA-A2 molecule.

3.2. Recognition of Tax11-19 peptide by CTL lines of different avidity

Based on the observation that Tax11-19 showed strong antigenicity inducing specific CTLs, we next attempted to develop low-avidity CTLs (LCTL) and high-avidity CTLs (HCTL) from HLA-A2 transgenic mice. HCTL were generated by weekly stimulation using low concentrations (10 nM) of the Tax peptide pulsed onto APCs, while LCTLs were also generated using 10 μM of the Tax peptide pulsed onto APCs. Using these different CTL lines, we examined Tax-specific CTLs-mediated cytotoxicity with Tax peptide titrated over a range of concentrations. The titration curve showed a

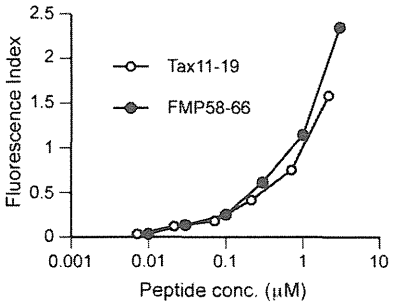

Fig. 1. Comparison of HLA-A2 binding curves between Tax11-19 and FMP58-66 peptide in T2-binding assay. The binding affinity of Tax11-19 for HLA-A2 molecule is almost as strong as that of FMP58-66 in influenza A virus.

0.5–1 $\log_{10}$ difference in functional avidity measured as the peptide concentration necessary to produce 50% lysis (Fig. 2A). Similarly, we examined their properties in antigen-specific IFN-γ production from these CTL lines (Fig. 2B). With a 24 h assay, HCTLs showed more IFN-γ production than LCTLs even at lower concentration of Tax antigen. These data suggest that the two different CTL lines specific for Tax have different functional avidity.

3.3. Different Vβ usage and binding ability to Tax-tetramer between high- and low-avidity CTLs

In order to confirm whether these CTLs with different avidity possessed different TCR structures, we assessed the difference in Vβ usage pattern between HCTLs and LCTLs using flow cytometric analysis (FCM). On FCM, antibodies available for screening were those for Vβ 2, 3, 4, 5, 6, 7, 8.1, 8.2, 8.3, 9, 10, 11, 12, 13, 14, and 17. On FCM, no Vβ were detected in LCTLs, while only Vβ5 was detected in HCTLs (Fig. 3A). The data suggested that the major TCR repertoire of HCTL is Vβ5, indicating that these two Tax-specific CTL lines have different TCR structures.

We next compared the binding affinity of TCR between HCTL and LCTL using Tax11-19/HLA-A2 tetramer-LLFGYPVYV and anti-CD3 Ab (Fig. 3B). On FCM with both Tax11-19-tetramer and anti-CD3 Ab titration, HCTLs showed a stronger fluorescence than LCTLs (Fig. 3B). On Tax11-19-tetramer assay, the ratio of fluorescence index (HCTL/LCTL) was ~5-fold at any titrated concentration, and it took 1.5 logs more tetramer to achieve the same level of staining. In the titration of anti-CD3 Ab, the ratio was ~3-fold and also it required about 3-fold more antibody to reach the same level of staining. These findings suggested that HCTLs not only have higher TCR affinity but also express greater numbers of TCR molecules on their surface when compared with LCTLs.

3.4. Recognition of human ATL targets by Tax-specific CTLs from HHD mice

We further examined whether these murine CTL lines with different functional avidity could induce cytotoxic activity against human ATL targets. We used the HTLV-1-infected human ATL cell lines, KK-1 (HLA-A2) and KOB (HLA-A30) as target cells derived from peripheral blood and ascitis of ATL patients, respectively [23,24]. These murine CTL lines did not show strong cytotoxicity against human ATL lines as against murine targets with a 4 h assay, as it was previously reported that species specificity between murine CD8 and the α3 domain of human HLA-A2 may reduce the recognition ability by CTLs [33]. However, on a 12 h assay, cytotoxicity against human ATL was observed in an HLA-A2 restricted manner (Fig. 4A). HCTLs were especially more efficient at killing at low E/T ratios. Furthermore, on kinetics assay, HCTLs showed more efficient cytotoxicity against the human ATL target (KK-1) than LCTLs (Fig. 4B).

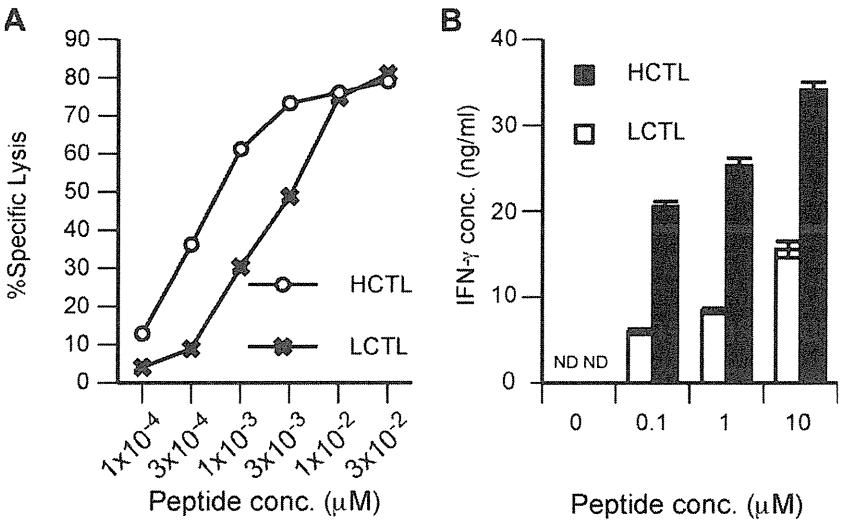

Fig. 2. Difference in functional avidity between HCTLs and LCTLs. (A) Recognition by the Tax11-19 peptide specific CTLs, HCTL and LCTL, of Tax11-19 antigenic peptide from 10^{-4} to 10 μM when presented on C1R.AAD target cells. The effector to target-cell (E/T) ratio was 20:1. Error bars were omitted because all SEMs were <3.5%. (B) Comparison of Tax11-19-specific IFN-γ production between HCTLs and LCTLs. A total of 200,000 CTL cells were cultured with 100,000 mytomicin-c treated C1R.AAD cell with 0.1–10 μM Tax11-19 peptide. Culture supernatants at 24 h were assayed using IFN-γ ELISA kit according to the manufacturer's instructions. ND, not detected.

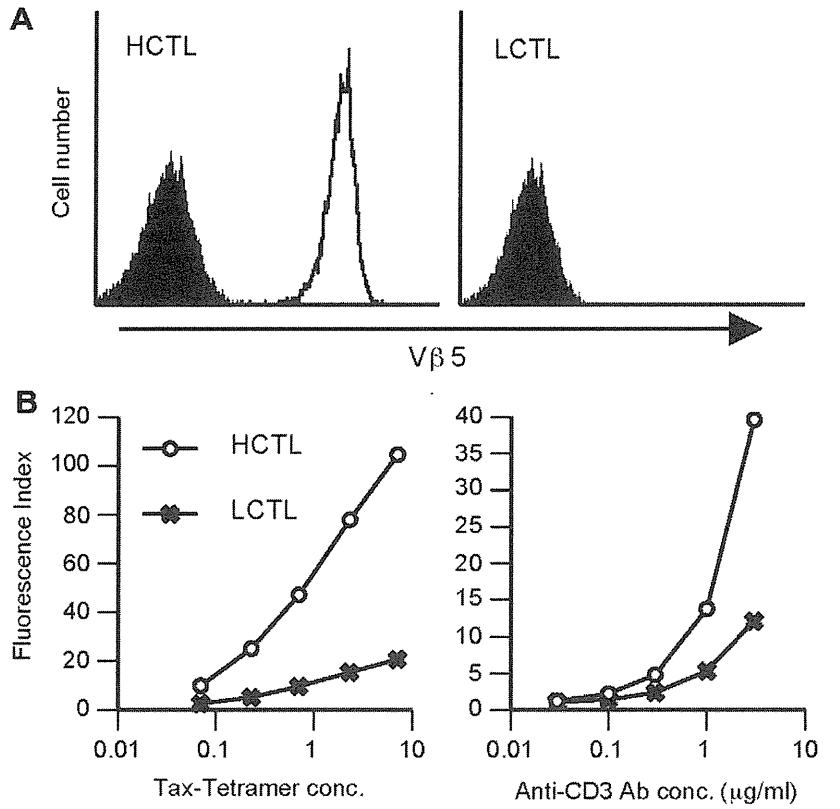

Fig. 3. TCR Vβ usage and expression level of TCR complex on Tax-specific CTLs with different functional avidity. (A) Comparison of Vβ usage pattern between HCTLs and LCTLs cytometry analysis (FCM). No Vβs among available anti-Vβ antibodies were detected in LCTL but only Vβ5 was detected in HCTL. (B) Comparison of binding curves for human Tax11-19-tetramer and anti-CD3ε Ab between HCTLs and LCTLs. HCTLs consistently showed a stronger fluorescence index than LCTLs; for Tax11-19-tetramer, the ratio of fluorescence index (LCTL/HCTL) was ~5-fold, and for anti-CD3ε Ab, it was ~3-fold.

3.5. Recognition of HTLV-1 infected human T cells by Tax-specific CTL from HHD mice

Next, in order to examine a comparison of the cytotoxicity against HTLV-1 infected non-tumor cells, we used HTLV-1 infected human T cells (HCT-4) derived from a patient with HAM/TSP [25]. On a 12 h lytic assay, HCTLs showed more efficient cytotoxicity against the HTLV-1 infected human T cells while LCTLs were not able to kill the targets under the these experimental conditions (Fig. 5A). At no time point was there detectable killing by LCTLs (Fig. 5B). These findings suggested that the superior recognition ability by the CTLs with higher functional avidity may have a more

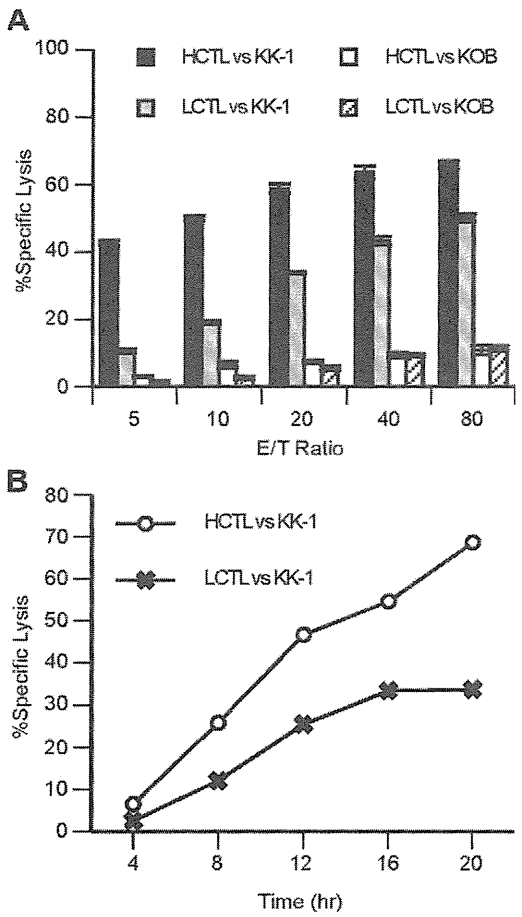

Fig. 4. Recognition pattern of human ATL targets by Tax-specific CTLs. (A) Comparison of cytotoxicity for human ATL targets (KK1, HLA-A2; KOB, HLA-A30) between HCTLs and LCTLs. (12 h ^{51}Cr release assay) (B) Comparison of kinetics of Tax-specific CTL-mediated cytotoxicity (E:T ratio = 40:1) between HCTLs and LCTLs. Similar results were obtained in three different experiments.

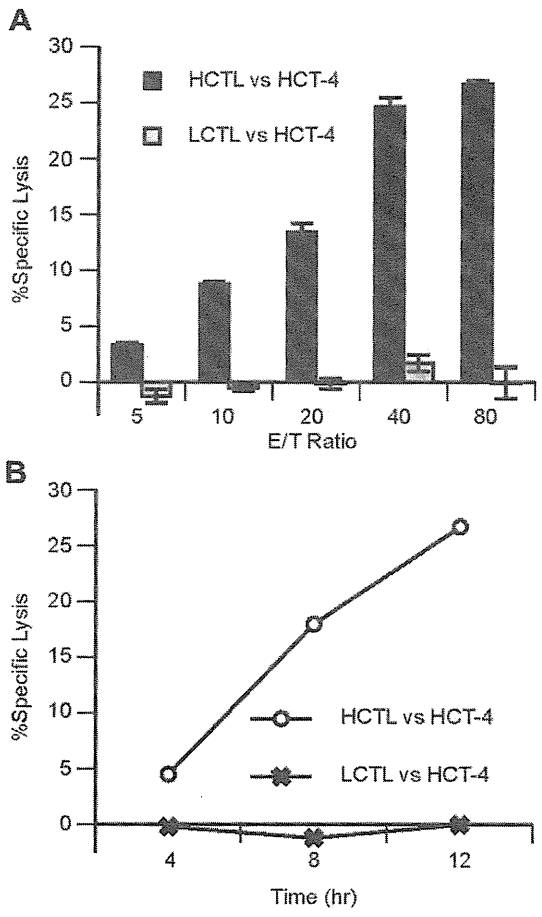

Fig. 5. Recognition pattern of HTLV-1 infected human T cell line by Tax-specific CTLs. (A) Comparison of cytotoxicity for human IL-2 dependent HTLV-1 infected cell, HCT-4 (HLA-A2), between HCTLs and LCTLs. (12 h ^{51}Cr release assay). (B) Comparison of kinetics of Tax-specific CTL-mediated cytotoxicity (E:T = 40:1) between HCTLs and LCTLs. Similar results were obtained in four different experiments.

striking effect in the case of recognizing normal cells infected with the virus.

3.6. Expression of Tax product in human ATL tumors and HTLV-1 infected T cell target

The cytotoxicity data against human targets indicated that higher functional avidity in CTLs is critical for efficient cytotoxicity against tumor or infected normal cell targets in humans. However, the amount of Tax antigen expressed in target cells that could be recognized by higher avidity CTLs was unclear. Therefore, we investigated how much Tax products could be yielded in these human ATL and HTLV-1 infected target cells. Using western blotting (Fig. 6A), Tax protein was detected in KOB and HCT-4 target cells, but not in KK-1. Since KK-1 cells were recognized by HCTLs more strongly than by LCTLs, we further evaluated the level of Tax mRNA produced in KK-1 using real-time PCR. The expression levels of Tax mRNA in KK-1 were around one thousand-fold lower than that in KOB (Fig. 6B). These results demonstrated that Tax11-19-specific higher avidity CTLs showed more efficient cytotoxicity against ATL by recognizing very small amount of Tax product detected only with real-time PCR.

4. Discussion

HTLV-1 infection elicits a strong CTL response, with Tax protein being the major target of HTLV-1-specific CTLs [10,11]. In the field of anti-tumor immunity, the in vivo relevance of differences in functional avidity has been established by demonstrating that high-avidity CTLs clear tumor antigens more efficiently than low-avidity CTL [34–38]. In HTLV-1 infection, however, while there is increasing body of evidence that CTL quality from the aspect of functional avidity of CTL might be crucial for the efficient control of HTLV-1 infection [17,39], little is known about how the functional avidity of HTLV-1 virus-specific CTLs is related to the control of HTLV-1-infected cells and tumors. Furthermore, the virus is latent in the tumor cells and it is difficult to detect expression of viral proteins [40–42]. This is the reason why there has not been direct evidence on whether Tax11-19 works as a definitive CTL antigen in HLA-A2-restricted patients with HTLV-1 infection and ATLs. The present study provides clear evidence regarding the notion that high avidity CTLs specific for Tax protein play a greater role in the specific destruction of ATL and HTLV-1-infected cells using Tax-specific CTLs with different functional avidity generated from HLA-A2 transgenic HHD mice, with human ATL lines and HTLV-1 infected cells acting as targets. As Tax11-19 peptide antigen binds HLA-A2 with almost as high affinity as FMP58-66 in influenza A virus (Fig. 1), which has one of the highest affinity peptides among HLA-A2 restricted peptide antigens [27,28], we developed CTL lines specific for Tax11-19, HCTL and LCTL, for which we found the optimum antigen-presenting conditions for the induction and maintenance of the CTL lines were 10 nM- and

10 μM-peptide pulsing APCs, respectively. The 1000-fold difference of such antigenic concentration resulted in the CTL lines with differences of functional avidity in antigen-specific cytotoxicity and IFN-γ production (Fig. 2). These different avidity CTLs also had different repertoires of TCRVβ, suggesting the structure of TCR in the major repertoire of two lines were distinct (Fig. 3A). In order to compare TCR affinity for the human Tax-tetramer, the mismatch of which to murine CD8 could permit assessment of the strength of TCR ligation to peptide/MHC complex more closely without the influence of CD8 binding [43], we titrated the tetramer and evaluated the effect of the number of TCR molecules expressed at the same time. Higher avidity Tax-specific CTLs showed higher fluorescene on both Tax-tetramer (~5-fold) and anti-CD3Ab (~3-fold) staining (Fig. 3B), thus suggesting that CTL might acquire higher avidity state by possessing the different structure of the TCR as well as by increasing the number of TCR molecules expressed although other factors could also play a role for determining the avidity of CTLs [15].

HTLV-1 Tax, a critical viral protein for HTLV-1 leukemogenesis, is the most likely target for HTLV-1 specific CTL in HTLV-1-infected individuals [10,11]. In HTLV-1-infected patients with HLA-A2, the Tax11-19-specific CTL response is predominantly detected in culture [44]. However, few details are known about the recognition mechanism by Tax-specific CTLs because of the difficulty of developing CTL lines specific for Tax11-19 antigen [9]. Although both HCTLs and LCTLs developed from HLA-A2 transgenic mice were not able to induce cytotoxicity against the human HLA-A2-restricted ATL line, KK-1, on 4 h assay because of the mismatch between the murine CD8 and human α3 domain [22], HCTLs clearly showed more efficient cytotoxicity than LCTLs with longer-term assay of more than 4 h (Fig. 4). Furthermore, the use of the human IL-2-dependent HTLV-1-infected non-tumor cell, HCT-4, clearly brought out the difference in cytotoxic efficacy between HCTL and LCTL (Fig. 5). These findings could be direct evidence not only that Tax11-19 might be naturally processed for presentation as a CTL antigen in both ATL tumor cells and virus-infected cells but also that the higher avidity CTL for Tax11-19 could be more critical in clearing HTLV-1-infected cells as well as ATL tumors in HLA-A2-restricted patients. In addition, HCTLs could more strongly recognize a latent level of Tax product detected only with a real-time PCR, not detectable with western blotting in the ATL target (Fig. 6). Furthermore, HCTLs also possessed higher elimination potential against HTLV-1 infected non-tumor targets when compared with LCTLs (Figs. 4 and 5).

The present findings are consistent with previous reports showing that the lytic efficiency of $CD8^+$ T cell response was inversely correlated with the proviral load and the rate of proviral expression in patients with HTLV-1 infection [17]. These data also strongly support the notion that induction of high avidity CTLs is critical for development of more effective vaccines against cancer and chronic viral infection such as HTLV-1and HIV. In addition, based on the observation that the high-avidity CTLs expressed a greater number of TCR molecules when compared with the low-avidity CTLs (Fig. 3B), such more multivalent TCR display might be one of the critical factors in establishing functional high avidity, leading to more efficient TCR cell therapy in the future [45].

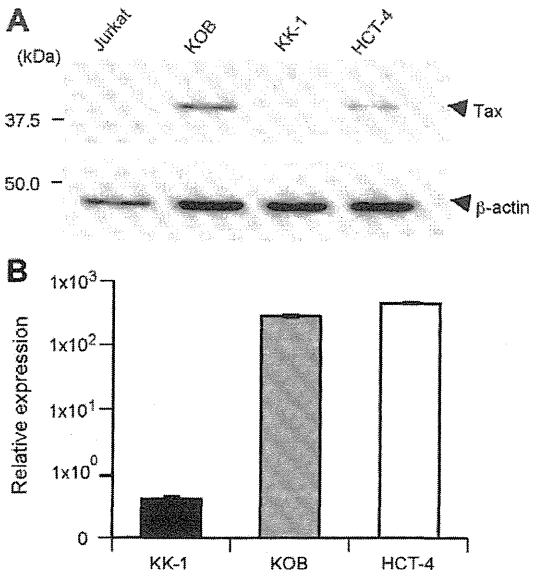

Fig. 6. Expression of Tax product in human ATL tumors and HTLV-1 infected T cell targets. (A) Tax protein is detected in KOB and HCT-4 by western blotting, but not in KK-1. Jurkat cells were used as a negative control. (B) Comparison of mRNA production of Tax by real-time PCR among KOB, KK-1 and HCT-4. Tax production in KK-1 was detected by real-time PCR, but not in a western blotting. Jurkat cells as a negative control gave no detectable signal with the Tax-primer.

Conflict of interest

The authors declare no conflict of interest.

Acknowledgments

We would like to thank Dr. Jay A. Berzofsky for critical reading of the manuscript and helpful suggestions. We also would like to thank Hiroe Ogasawara and Katsunori Takahashi for technical assistance provided during the study.

References

[1] Y. Hinuma, K. Nagata, M. Hanaoka, M. Nakai, T. Matsumoto, K.I. Kinoshita, S. Shirakawa, I. Miyoshi, Adult T-cell leukemia: antigen in an ATL cell line and detection of antibodies to the antigen in human sera, Proc. Natl. Acad. Sci. USA 78 (1981) 6476–6480.
[2] M. Yoshida, M. Seiki, K. Yamaguchi, K. Takatsuki, Monoclonal integration of human T-cell leukemia provirus in all primary tumors of adult T-cell leukemia suggests causative role of human T-cell leukemia virus in the disease, Proc. Natl. Acad. Sci. USA 81 (1984) 2534–2537.
[3] A. Gessain, F. Barin, J.C. Vernant, O. Gout, L. Maurs, A. Calender, G. De The, Antibodies to human T-lymphotropic virus type-I in patients with tropical spastic paraparesis, Lancet 2 (1985) 407–410.
[4] M. Osame, K. Usuku, S. Izumo, N. Ijichi, H. Amitani, A. Igata, M. Matsumoto, M. Tara, HTLV-I associated myelopathy, a new clinical entity, Lancet 1 (1986) 1031–1032.
[5] T. Matsuzaki, M. Nakagawa, M. Nagai, K. Usuku, I. Higuchi, K. Arimura, H. Kubota, S. Izumo, S. Akiba, M. Osame, HTLV-I proviral load correlates with progression of motor disability in HAM/TSP: analysis of 239 HAM/TSP patients including 64 patients followed up for 10 years, J. Neurovirol. 7 (2001) 228–234.
[6] M.A. Nowak, C.R. Bangham, Population dynamics of immune responses to persistent viruses, Science 272 (1996) 74–79.
[7] A.M. Vine, A.G. Heaps, L. Kaftantzi, A. Mosley, B. Asquith, A. Witkover, G. Thompson, M. Saito, P.K. Goon, L. Carr, F. Martinez-Murillo, G.P. Taylor, C.R. Bangham, The role of CTLs in persistent viral infection: cytolytic gene expression in CD8+ lymphocytes distinguishes between individuals with a high or low proviral load of human T cell lymphotropic virus type 1, J. Immunol. 173 (2004) 5121–5129.
[8] M. Kannagi, K. Sugamura, K. Kinoshita, H. Uchino, Y. Hinuma, Specific cytolysis of fresh tumor cells by an autologous killer T cell line derived from an adult T cell leukemia/lymphoma patient, J. Immunol. 133 (1984) 1037–1041.
[9] B. Arnulf, M. Thorel, Y. Poirot, R. Tamousa, E. Boulanger, A. Jaccard, E. Oksenhendler, O. Hermine, C. Pique, Loss of the ex vivo but not the reinducible CD8+ T-cell response to Tax in human T-cell leukemia virus type 1-infected patients with adult T-cell leukemia/lymphoma, Leukemia 18 (2004) 126–132.
[10] S. Jacobson, H. Shida, D.E. McFarlin, A.S. Fauci, S. Koenig, Circulating CD8+ cytotoxic T lymphocytes specific for HTLV-I pX in patients with HTLV-I associated neurological disease, Nature 348 (1990) 245–248.
[11] M. Kannagi, S. Harada, I. Maruyama, H. Inoko, H. Igarashi, G. Kuwashima, S. Sato, M. Morita, M. Kidokoro, M. Shigemoto, Predominant recognition of human T cell leukemia virus type I (HTLV-I) pX gene products by human CD8+ cytotoxic T cells directed against HTLV-I-infected cells, Int. Immunol. 3 (1991) 761–767.

[12] K.T. Jeang, Functional activities of the human T-cell leukemia virus type I Tax oncoprotein: cellular signaling through NF-kappa B, Cytokine Growth Factor Rev. 12 (2001) 207–217.
[13] M. Yoshida, Multiple viral strategies of HTLV-1 for dysregulation of cell growth control, Annu. Rev. Immunol. 19 (2001) 475–496.
[14] M. Kannagi, S. Matsushita, S. Harada, Expression of the target antigen for cytotoxic T lymphocytes on adult T-cell-leukemia cells, Int. J. Cancer 54 (1993) 582–588.
[15] M.A. Alexander-Miller, High-avidity CD8+ T cells: optimal soldiers in the war against viruses and tumors, Immunol. Res. 31 (2005) 13–24.
[16] M. Derby, M. Alexander-Miller, R. Tse, J.A. Berzofsky, High-avidity CTL exploit two complementary mechanisms to provide better protection against viral infection than low-avidity CTL, J. Immunol. 166 (2001) 1690–1697.
[17] T. Kattan, A. MacNamara, A.G. Rowan, et al., The avidity and lytic efficiency of the CTL response to HTLV-1, J. Immunol. 182 (9) (2009) 5723–5729.
[18] A. Gallimore, T. Dumrese, H. Hengartner, R.M. Zinkernagel, H.G. Rammensee, Protective immunity does not correlate with the hierarchy of virus-specific cytotoxic T cell responses to naturally processed peptides, J. Exp. Med. 187 (1998) 1647–1657.
[19] A.G. Cawthon, H. Lu, M.A. Alexander-Miller, Peptide requirement for CTL activation reflects the sensitivity to CD3 engagement: correlation with CD8ab versus CD8aa expression, J. Immunol. 167 (2001) 2577–2584.
[20] S. Walter, L. Herrgen, O. Schoor, G. Jung, D. Wernet, H.J. Buhring, H.G. Rammensee, S. Stevanovic, Cutting edge: predetermined avidity of human CD8 T cells expanded on calibrated MHC/anti-CD28-coated microspheres, J. Immunol. 171 (2003) 4974–4978.
[21] P.M. Gray, G.D. Parks, M.A. Alexander-Miller, High avidity CD8+ T cells are the initial population elicited following viral infection of the respiratory tract, J. Immunol. 170 (2003) 174–181.
[22] M.H. Newberg, D.H. Smith, S.B. Haertel, D.R. Vining, E. Lacy, V.H. Engelhard, Importance of MHC class 1 a2 and a3 domains in the recognition of self and non-self MHC molecules, J. Immunol. 156 (1996) 2473–2480.
[23] Y. Yamada, Y. Nagata, S. Kamihira, M. Tagawa, M. Ichimaru, M. Tomonaga, H. Shiku, IL-2-dependent ATL cell lines with phenotypes differing from the original leukemia cells, Leuk. Res. 15 (1991) 619–625.
[24] T. Maeda, Y. Yamada, R. Moriuchi, K. Sugahara, K. Tsuruda, T. Joh, S. Atogami, K. Tsukasaki, M. Tomonaga, S. Kamihara, Fas gene mutation in the progression of adult T cell leukemia, J. Exp. Med. 189 (1999) 1063–1071.
[25] N. Fukushima, Y. Nishiura, T. Nakamura, Y. Yamada, S. Kohno, K. Eguchi, Involvement of p38 MAPK signaling pathway in IFN-g and HTLV-I expression in patients with HTLV-I-associated myelopathy/tropical spastic paraparesis, J. Neuroimmunol. 159 (2005) 196–202.
[26] S. Pascolo, N. Bervas, J.M. Ure, A.G. Smith, F.A. Lemonnier, B. Perarnau, HLA-A2.1-restricted education and cytolytic activity of CD8(+) T lymphocytes from b2 microglobulin (b2m) HLA-A2.1 monochain transgenic H-2Db b2m double knockout mice, J. Exp. Med. 185 (1997) 2043–2051.
[27] T. Okazaki, C.D. Pendleton, F. Lemonnier, J.A. Berzofsky, Epitope-enhanced conserved HIV-1 peptide protects HLA-A2-transgenic mice against virus expressing HIV-1 antigen, J. Immunol. 171 (2003) 2548–2555.
[28] T. Okazaki, M. Terabe, A.T. Catanzaro, C.D. Pendleton, R. Yarchoan, J.A. Berzofsky, Possible therapeutic vaccine strategy against human immunodeficiency virus escape from reverse transcriptase inhibitors studied in HLA-A2 transgenic mice, J. Virol. 80 (2006) 10645–10651.
[29] A. Maeda, T. Okazaki, M. Inoue, T. Kitazono, M. Yamasaki, F.A. Lemonnier, S. Ozaki, Immunosuppressive effect of angiotensin receptor blocker on stimulation of mice CTLs by angiotensin II, Int. Immunopharmacol. 9 (2009) 1183–1188.
[30] B. Lee, Y. Tanaka, H. Tozawa, Monoclonal antibody defining tax protein of human T-cell leukemia virus type-I, Tohoku J. Exp. Med. 157 (1989) 1–11.
[31] Y. Yamano, N. Araya, T. Sato, A. Utsunomiya, K. Azakami, D. Hasegawa, T. Izumi, H. Fujita, S. Aratani, N. Yagishita, R. Fujii, K. Nishioka, S. Jacobson, T. Nakajima, Abnormally high levels of virus-infected IFN-g+ CCR4+ CD4+ CD25+ T cells in a retrovirus-associated neuroinflammatory disorder, PLoS ONE 4 (2009) e6517.
[32] F. Gotch, J. Rothbard, K. Howland, A. Townsend, A. McMichael, Cytotoxic T lymphocytes recognize a fragment of influenza virus matrix protein in association with HLA-A2, Nature 326 (1987) 881–882.
[33] M.H. Newberg, J.P. Ridge, D.R. Vining, R.D. Salter, V.H. Engelhard, Species specificity in the interaction of CD8 with the a3 domain of MHC class I molecules, J. Immunol. 149 (1992) 136–142.
[34] M.A. Alexander-Miller, G.R. Leggatt, J.A. Berzofsky, Selective expansion of high- or low-avidity cytotoxic T lymphocytes and efficacy for adoptive immunotherapy, Proc. Natl. Acad. Sci. USA 93 (1996) 4102–4107.
[35] C. Sedlik, G. Dadaglio, M.F. Saron, E. Deriaud, M. Rojas, S.I. Casal, C. Leclerc, In vivo induction of a high-avidity, high-frequency cytotoxic T-lymphocyte response is associated with antiviral protective immunity, J. Virol. 74 (2000) 5769–5775.
[36] V. Dutoit, V. Rubio-Godoy, P.Y. Dietrich, A.L. Quiqueres, V. Svhnuriger, D. Rimoldi, D. Lienard, D. Speiser, P. Guillaume, P. Batard, J.C. Cerottini, P. Romero, D. Valmori, Heterogeneous T-cell response to MAGE-A10(254–262): high avidity-specific cytolytic T lymphocytes show superior antitumor activity, Cancer Res. 61 (2001) 5850–5856.
[37] C. Yee, P.A. Savage, P.P. Lee, M.M. Davis, P.D. Greenberg, Isolation of high avidity melanoma-reactive CTL from heterogeneous populations using peptide-MHC tetramers, J. Immunol. 162 (1999) 2227–2234.
[38] H.J. Zeh III, D. Perry-Lalley, M.E. Dudley, S.A. Rosenberg, J.C. Yang, High avidity CTLs for two self-antigens demonstrate superior in vitro and in vivo antitumor efficacy, J. Immunol. 162 (1999) 989–994.
[39] C.R. Bangham, CTL quality and the control of human retroviral infections, Eur. J. Immunol. 39 (2009) 1700–1712.
[40] H. Konishi, N. Kobayashi, M. Hatanaka, Defective human T-cell leukemia virus in adult T-cell leukemia patients, Mol. Biol. Med. 2 (1984) 273–283.
[41] T. Kinoshita, M. Shimoyama, K. Tobinai, M. Ito, S. Ito, S. Ikeda, K. Tajima, K. Shimotohno, T. Sugimura, Detection of mRNA for the tax1/rex1 gene of human T-cell leukemia virus type I in fresh peripheral blood mononuclear cells of adult T-cell leukemia patients and viral carriers by using the polymerase chain reaction, Proc. Natl. Acad. Sci. USA 86 (1989) 5620–5624.
[42] T. Uchiyama, Human T cell leukemia virus type I (HTLV-I) and human diseases, Annu. Rev. Immunol. 15 (1997) 15–37.
[43] E.M. Choi, J.L. Chen, L. Wooldridge, M. Salio, A. Lissina, N. Lissin, I.F. Hermans, J.D. Silk, F. Milza, M.J. Palmowski, P.R. Dumbar, B.K. Jacobson, A.K. Sewell, V. Cerundolo, High avidity antigen-specific CTL identified by CD8-independent tetramer staining, J. Immunol. 171 (2003) 5116–5123.
[44] M. Kannagi, H. Shida, H. Igarashi, K. Kuruma, H. Murai, Y. Aono, I. Maruyama, M. Osame, T. Hattori, H. Inoko, Target epitope in the Tax protein of human T-cell leukemia virus type I recognized by class I major histocompatibility complex-restricted cytotoxic T cells, J. Virol. 66 (1992) 2928–2933.
[45] C. Govers, Z. Sebestyen, M. Coccoris, R.A. Willemsen, R. Debets, T cell receptor gene therapy: strategies for optimizing transgenic TCR pairing, Trends Mol. Med. 16 (2010) 77–87.

J. Biochem. 2011;150(6):679–686 doi:10.1093/jb/mvr106

THE JOURNAL OF BIOCHEMISTRY

Activation of the IκB kinase complex by HTLV-1 Tax requires cytosolic factors involved in Tax-induced polyubiquitination

Received August 3, 2011; accepted August 13, 2011; published online August 23, 2011

Yuri Shibata[1], Yuetsu Tanaka[2], Jin Gohda[1] and Jun-ichiro Inoue[1,*]

[1]Department of Cancer Biology, Division of Cellular and Molecular Biology, Institute of Medical Science, University of Tokyo, Shirokane-dai, Minato-ku, Tokyo 108-8639; and [2]Department of Immunology, Faculty of Medicine, University of the Ryukyus, Nishihara, Okinawa 903-0213, Japan

*Jun-ichiro Inoue, Department of Cancer Biology, Division of Cellular and Molecular Biology, Institute of Medical Science, University of Tokyo, 4-6-1 Shirokane-dai, Minato-ku, Tokyo 108-8639, Japan. Tel: +81 3 5449 5275, Fax: +81 3 5449 5421, email: jun-i@ims.u-tokyo.ac.jp

Activation of NF-κB by human T cell leukaemia virus type 1 Tax is thought to be crucial in T-cell transformation and the onset of adult T cell leukaemia. Tax activates NF-κB through activation of the IκB kinase (IKK) complex, similar to cytokine-induced NF-κB activation, which involves active signalling complex formation using polyubiquitin chains as a platform. Although polyubiquitination of Tax was reported to be required for IKK activation, most studies have been performed using intact cells, in which secondary NF-κB activation can be induced by various cytokines that are secreted due to Tax-mediated primary NF-κB activation. Therefore, a cell-free assay system, in which IKK can be activated by adding highly purified recombinant Tax to cytosolic extract, was used to analyse Tax-induced IKK activation. In contrast to the cytosolic extract, the purified IKK complex was not activated by Tax, whereas, it was efficiently activated by MEKK1, that does not require polyubiquitination to activate IKK. Moreover, Tax-induced IKK activation was blocked when the cytosolic extract was mixed with either lysine-free, methylated or K63R ubiquitin. These results obtained through our cell-free assay suggest that K63-linked polyubiquitination is critical, but linear polyubiquitination is dispensable or insufficient for Tax-induced IKK activation.

Keywords: Human T cell leukaemia virus type 1/IκB kinase/NF-κB/polyubiquitination/Tax.

Abbreviations: ATL, Adult T-cell leukaemia; CYLD, cylindromatosis; HTLV-1, Human T cell leukaemia virus type 1; IKK, IκB kinase; MEKK1, MAPK/ERK kinase; NEMO, NF-κB essential modulator; NF-κB, nuclear factor-κB; TRAF6, TNF receptor-associated factor 6.

Human T-cell leukaemia virus type 1 (HTLV-1) infects and transforms $CD4^+$ T cells *in vitro* and is etiologically associated with an acute T cell malignancy, Adult T-cell leukaemia (ATL) (*1*). The HTLV-1 genome encodes the Tax protein, which plays a critical role in T-cell transformation (*2*, *3*). Tax regulates the expression of cellular genes involved in T-cell proliferation, cell survival and anti-apoptosis by modulating various transcription factors, including nuclear factor-κB (NF-κB), cAMP-responsible element binding protein (CREB) and serum response factor (SRF) (*1*, *4*). NF-κB is one of the key transcription factors that facilitate cell transformation because the Tax mutant M22, which can activate CREB but not NF-κB, is unable to immortalize T cells (*5*). Therefore, elucidation of the mechanism that underlies Tax-induced NF-κB activation may aid in preventing the onset of ATL.

NF-κB is normally sequestered in the cytoplasm by associating with inhibitory proteins from the NF-κB family (IκBs). Extracellular stimuli, such as tumour necrosis factor (TNF)-α and interleukin (IL)-1, activate the IκB kinase (IKK) complex, that is composed of the catalytic subunits IKKα and IKKβ and the regulatory subunit NF-κB essential modulator (NEMO). The activated IKK complex phosphorylates IκBα, which, in turn, induces Lys48-linked polyubiquitination and proteasomal degradation of IκBα. NF-κB is then translocated into the nucleus and promotes transcription of its target genes (*6*). It has been well established that Lys63-linked polyubiquitination is involved in the cytokine-mediated NF-κB activation pathway (*7*). In the interleukin-1 receptor (IL-1R) and Toll-like receptor (TLR) signalling pathways, TNF receptor (TNFR)-associated factor 6 (TRAF6), an E3 ubiquitin ligase, conjugates Lys63-linked polyubiquitination to itself and TGF-β-activated kinase (TAK) 1 together with Ubc13, an E2 ubiquitin-conjugating enzyme (*8*, *9*). Polyubiquitination leads to formation of a signalling complex that contains MAPK/ERK kinase (MEKK3), TAK1, TAK1-binding (TAB) 2/TAB3 and the IKK complex, which induces activation of TAK1 and the IKK complex (*10*). In TNFR1 signalling, cIAPs act as an E3 ubiquitin ligase that conjugates polyubiquitin chains to receptor-interacting protein (RIP) 1 (*11*, *12*). Polyubiquitin chains that are conjugated to RIP1 also act as platforms for the formation of a signalling complex to activate downstream molecules.

To date, many studies have been conducted to elucidate the mechanism of Tax-induced IKK activation. Tax binds to NEMO and induces activation of the IKK complex (*13*, *14*). We have shown that, unlike the cytokine-mediated NF-κB signalling pathway, Tax does not require Ubc13 and MAP3Ks, including TAK1, MEKK1, MEKK3, NF-κB-inducing kinase (NIK) and tumor progression locus (TPL)-2 for IKK

activation (*15*). We have further shown that expression of cylindromatosis (CYLD) does not affect Tax-induced NF-κB activation, whereas it does inhibit TRAF6-induced NF-κB activation (*15*), which led us to hypothesize that polyubiquitination may not be required for Tax-induced NF-κB activation. However, other groups have shown that Ubc13 and TAK1 are required for Tax-induced NF-kB activation (*16*). Therefore, the molecular mechanisms for Tax-induced IKK activation are controversial and largely unknown.

Herein, we establish a cell-free assay system that induces IKK activation in response to recombinant Tax and demonstrate that Tax requires unidentified cytosolic factor(s) to activate the purified IKK complex. We further show that a ubiquitin mutant, which is unable to form polyubiquitin chains, inhibit activation of the IKK complex, which suggests that polyubiquitination is involved in the Tax-induced IKK activation pathway.

Experimental Procedures

Plasmids

The cDNAs that encode Tax, M22, TRAF6, MEKK1 (the C-terminal 321 amino acids) were inserted into the pFastBac™ HT A vector (Invitrogen) to generate a recombinant baculovirus for expression of these proteins in Sf9 cells.

Cell culture and reagents

The Jurkat and JM4.5.2 cells were maintained in RPMI 1640 with 10% heat-inactivated fetal bovine serum (FBS). The Sf9 cells were maintained in Sf900™ II SFM (Gibco) with 10% heat-inactivated FBS. Wild-type (WT) and *Traf6*$^{-/-}$ mouse embryonic fibroblasts (MEFs) (*17*) were maintained in Dulbecco's modified Eagle's medium (DMEM) with 10% heat-inactivated FBS. BAY 11-7082 and BMS-345541 were obtained from Calbiochem. The wild-type ubiquitin and ubiquitin mutants were purchased from Boston Biochem.

Purification of the recombinant proteins

His_6-tagged Tax, M22, TRAF6 and MEKK1 were produced using the Bac-to-Bac Baculovirus Expression System (Invitrogen). Briefly, a 50-ml culture of Sf9 cells (1×10^6 cells/ml) was infected with a recombinant baculovirus that expressed each protein. On completing 72 h after infection, the cells were harvested, and the His_6-tagged recombinant proteins were purified using the Ni-NTA resin (QIAGEN) according to the manufacturer's instructions.

Preparation of cytosolic extract (S100) from Jurkat cells

The Jurkat cells (1.5×10^8 cells) were resuspended in 500 µl of hypotonic buffer [10 mM Tris–HCl (pH 7.5), 1.5 mM $MgCl_2$, 10 mM KCl, 0.5 mM dithiothreitol (DTT) and a protease inhibitor cocktail (Roche)] and homogenized using a Dounce homogenizer. The cell debris was removed by ultracentrifugation at 100,000*g* for 1 h, and the cleared supernatant (S100) was collected.

Cell-free assay for IKK activation

The Jurkat cytosolic extract (10 mg/ml) was incubated with the indicated amount of either recombinant Tax, M22, TRAF6 or MEKK1 in ATP buffer [50 mM Tris–HCl (pH 7.5), 5 mM $MgCl_2$, 2 mM ATP, 5 mM NaF, 20 mM β-glycerophosphate, 1 mM Na_3VO_4 and a protease inhibitor cocktail]. After incubation at 30°C for 1 h, the reaction mixtures were immunoblotted, immunoprecipitated or pulled down. For the cell-free assay using the purified IKK complex, the IKK complex was immunoprecipitated with an anti-Flag antibody from Jurkat cells that stably expressed Flag-NEMO (5.0×10^8 cells). The purified IKK complex was incubated with the indicated recombinant proteins in the presence of 100 ng of GST-IκBα (amino acids 1–54) in ATP buffer.

Immunoblotting

Either the immunoprecipitates or the whole-cell lysates were separated by sodium dodecyl sulfate–polyacrylamide gel electrophoresis (SDS–PAGE) and transferred to a polyvinylidenedifluoride (PVDF) membrane (Millipore). The membranes were incubated with the appropriate primary antibodies. Immunoreactive proteins were visualized with anti-rabbit or anti-mouse IgG conjugated to horseradish peroxidase (Amersham Biosciences), followed by processing with an enhanced chemiluminescence (ECL) detection system (Amersham Biosciences). The following antibodies were used: anti-p-IκBα (9246), anti-IκBα (9242), anti-p-IKKα/IKKβ (2681), anti-IKKα (2682), anti-IKKβ (2684) and anti-NEMO (2695) from Cell Signaling Technology as well as ubiquitin (sc-8017) (Santa Cruz Biotechnology), anti-Tubulin (CP06) (Calbiochem), anti-His-tag (PM032) (MBL) and anti-Tax (Lt-4).

Pull-down assay and immunoprecipitation

For the pull-down assays, pull down buffer [10 mM Tris–HCl [pH 7.0], 150 mM NaCl, 0.5 mM ethylenediaminetetraacetic acid (EDTA), 1% NP-40, 10 mM imidazole] and Ni-NTA resin were added to an *in vitro* assay reaction mixture. After incubation at 4°C for 1 h, the Ni-NTA resin was washed three times with the pull-down buffer and immunoblotted. To detect polyubiquitination of Tax and NEMO, the reaction mixtures were boiled for 10 min with 1% SDS to remove non-covalently attached proteins. The reaction mixtures were diluted 10-fold in Tris/NaCl/EDTA (TNE) buffer [20 mM Tris–HCl (pH 7.5), 150 mM NaCl, 2 mM EDTA, 1% NP-40, 5 mM *N*-ethylmaleimide and a protease inhibitor cocktail] to reduce the concentration of SDS to 0.1%. The reaction mixtures were then incubated with antibodies against Tax or NEMO. The immunoprecipitates were washed three times with TNE buffer and immunoblotted using an anti-Ub antibody.

Results and Discussion

Establishment of a cell-free assay system that reproduces Tax-induced IKK complex activation

Once Tax activates NF-κB, various cytokines, including TNF-α and IL-1, may be induced by NF-κB and secreted, which in turn further activates NF-κB through the cytokine-specific receptors on the Tax-expressing cells (*18*, *19*). This potential autocrine-stimulated NF-κB activation enhances the difficulty of distinguishing signalling events induced by Tax from those induced by cytokines. Therefore, we tried to establish an *in vitro* cell-free system, in which Tax-induced IKK activation can be analysed without cytokine-induced IKK activation. The involvement of polyubiquitination in Tax-induced IKK activation is unclear, although its involvement in cytokine-induced IKK activation has been established (*7*). Thus, the cell-free system is suitable to address the role of polyubiquitin chains in Tax-induced IKK activation. We first expressed recombinant His_6-Tax and the Tax mutant M22, which is defective in NF-κB activation, in Sf9 cells and purified them using Ni-NTA agarose (Fig. 1A) To examine whether recombinant Tax activates the IKK complex, the cytosolic extract was prepared from the human T cell line Jurkat and incubated with either recombinant Tax or M22, and the resulting reaction mixture was analysed using immunoblots with anti-p-IκBα and anti-p-IKKα/β antibodies. Recombinant Tax, but not recombinant M22, induced phosphorylation of IκBα in a dose-dependent manner (Fig. 1B). Phosphorylation of IκBα was also indicated by the appearance of a slower migrating form of IκBα (Fig. 1B). Phosphorylation of IKKα/β was also

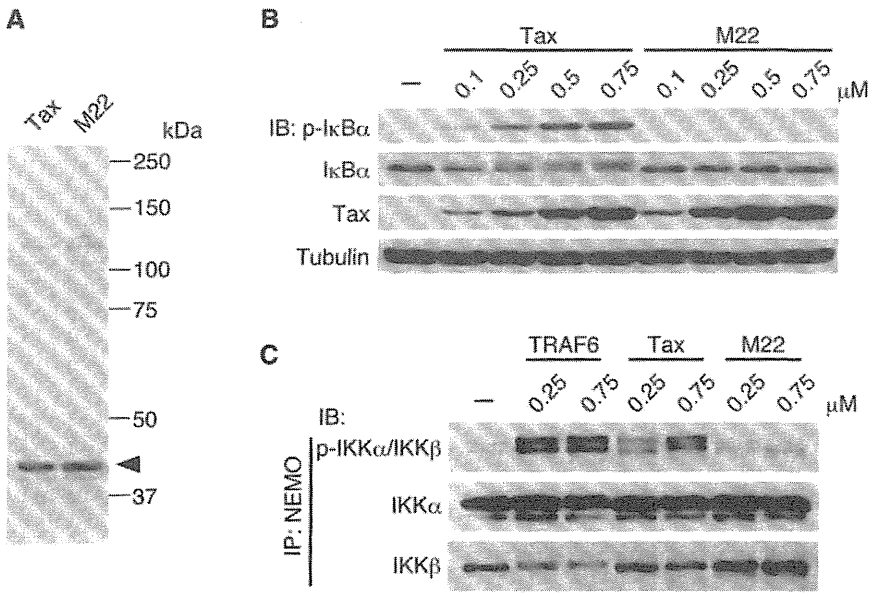

Fig. 1 Recombinant Tax activates the IKK complex in the cell-free assay system. (A) Purification of recombinant His_6-Tax and the Tax M22 mutant. We performed SDS–PAGE on the recombinant Tax and M22 that were purified from Sf9 cells, which was followed by silver staining. An arrow indicates the Tax protein. (B) Recombinant Tax induces phosphorylation of IκBα in a dose-dependent manner. The Jurkat cytosolic extract (10 mg/ml) was incubated with the indicated amount of recombinant either Tax or M22 with ATP (2 mM) at 30°C for 1 h. Phosphorylation of IκBα was detected by immunoblot with the anti-p-IκBα, anti-IκBα, anti-Tax and anti-Tubulin antibodies. (C) Recombinant Tax induces phosphorylation of the IKK complex. The Jurkat cytosolic extract (10 mg/ml) was incubated with the indicated amount of recombinant TRAF6, Tax or M22 at 30°C for 1 h. The reaction mixtures were immunoprecipitated with an anti-NEMO antibody and then immunoblotted with anti-p-IKKα/IKKβ, anti-IKKα and anti-IKKβ antibodies.

induced by recombinant Tax, but not by M22, to a similar extent as induced by TRAF6 (Fig. 1C).

To further confirm that recombinant Tax-induced phosphorylation of IκBα is catalysed by IKK, two distinct IKK inhibitors, BAY 11-7082 (*20*) and BMS-345541 (*21*), were added to the cell-free IKK activation system. Both of the IKK inhibitors inhibited Tax-induced phosphorylation of IκBα in a dose-dependent manner (Fig. 2A and B). Moreover, we performed the cell-free assay using cytosolic extract prepared from JM4.5.2, which is a NEMO-deficient Jurkat cell line, because the interaction of Tax with NEMO is indispensable to Tax-induced IKK activation (*22*, *23*). We confirmed that NEMO was not expressed in JM4.5.2 cells, whereas, IKKα and IKKβ were expressed to a similar extent in the JM4.5.2 and Jurkat cells (Fig. 2C, left). Previous study has shown that TRAF6 fails to induce IκBα phosphorylation in the absence of NEMO (*9*). While we reproduced the TRAF6 requirement for NEMO, recombinant Tax also failed to induce IκBα phosphorylation in the NEMO-deficient cytosolic extract (Fig. 2C, right). To examine whether Tax binding to the IKK complex depends on NEMO in the cell-free assay, Tax was pulled down with Ni-NTA beads, and IKKα/β binding to Tax was analysed by immunoblots. Recombinant Tax interacted with the IKK complex in the Jurkat cytosolic extract, whereas, Tax did not bind the IKK complex without NEMO (Fig. 2D). Taken together, Tax binds the IKK complex through NEMO and subsequently activates the IKK complex in the cell-free assay system. Given that M22, which is unable to bind NEMO (*14*), does not activate the IKK complex in the cell-free system (Fig. 1B and C), these results strongly suggest that our cell-free assay system reconstitutes the Tax-mediated NF-κB activation in intact cells. A similar assay system has been reported previously using partially purified recombinant Tax generated in *Escherichia coli* (*24*). As the purity of our Tax protein generated in sf9 cells is >95% (Fig. 1A) and its specific activity may be >8-fold over that of the Tax from *E. coli* [a minimum concentration of the Tax from Sf9 required for IKK activation is ~0.1 μM (Fig. 1B) while that of the Tax from *E. coli* is ~0.8 μM (*24*)], our system is well suited for further investigation of the molecular mechanism for Tax activation of NF-κB.

Tax requires cytosolic intermediary factors for activation of the purified IKK complex

Using the cell-free systems, we next addressed whether Tax alone induces IKK activation. The IKK complex was purified from unstimulated Jurkat cells and then incubated with either recombinant Tax or other NF-κB activators and recombinant GST-IκBα. As MEKK1 alone is known to activate the purified IKK complex without the polyubiquitination reaction (*9*, *25*), we used MEKK1 as a positive control. On the other hand, TRAF6 requires other molecules, such as Ubc13, Uev1a, TAK1 and TAB2, for IKK activation (*9*, *26*). Therefore, TRAF6 was used as a negative control. When incubated with Jurkat cytosolic extracts, all the recombinant proteins were able to induce phosphorylation of IκBα (Fig. 3A). However, when the recombinant proteins were incubated with the purified IKK complex, only MEKK1 induced phosphorylation of IκBα and IKKβ (Fig. 3B, +IKK).